environments

Article

Burn Severity and Environmental Controls of Postfire Forest Recovery in the Kostanay Region (Kazakhstan) Based on Integrated Field and Satellite Data

Zhanar Ozgeldinova [1], Altyn Zhanguzhina [1], Dana Akhmetova [1,*], Zhandos Mukayev [2,*], Meruyert Ulykpanova [3] and Karshyga Turluybekov [4]

[1] Department of Physical and Economic Geography, L.N. Gumilyov Eurasian National University, Astana 010008, Kazakhstan; ozgeldinova@mail.ru (Z.O.); altyn8828@mail.ru (A.Z.)
[2] Graduate School of Sports and Natural Sciences, Shakarim University, Semey 071400, Kazakhstan
[3] Department of History and Geography, Alikhan Bokeikhan University, Semey 071400, Kazakhstan; mikaulykpanova@mail.ru
[4] Semey Structural Division, RSE "Republican Forest Breeding and Seed Production Center", Semey 071400, Kazakhstan; karchi9494@gmail.com
* Correspondence: akhmetovadanaaa@mail.ru (D.A.); zhandos.mukaev@gmail.com (Z.M.); Tel.: +7-(707)-567-01-08 (D.A.); +7-(777)-706-23-85 (Z.M.)

Abstract

Wildfires are among the key drivers of transformation in boreal ecosystems; however, the mechanisms of postfire recovery in the arid regions of Eurasia remain insufficiently understood. The aim of this study was to identify the role of burn severity and associated edaphic and hydrological factors in shaping the natural regeneration trajectories of Scots pine forests in the Kostanay region of northern Kazakhstan. This study is based on the integration of field data on seedling regeneration and soil conditions with the analysis of long-term satellite-derived indices (NDVI, NDMI, and NBR). Sample plots were grouped according to fixed burn severity classes, which enabled a consistent statistical comparison and reduced the interpretative ambiguity that has characterized previous studies in the region. The results indicate that pine forest regeneration is most successful under low and moderate burn severity, where seed sources are preserved and favourable moisture conditions are maintained. In contrast, high burn severity leads to a reduction in regenerative potential and a shift in recovery trajectories toward deciduous or sparsely vegetated communities. The spectral indices derived from the remote sensing data strongly agreed with the field-based indicators, confirming their suitability for assessing postfire vegetation dynamics. Soil properties act as important modifying factors of recovery processes, particularly under conditions of limited water availability. These findings enhance the current understanding of postfire recovery mechanisms in the arid part of the boreal zone and highlight the need for differentiated management of postfire landscapes. The integration of field observations with remote sensing data provides a robust framework for monitoring and forecasting recovery processes under an increasingly intensified fire regime.

Keywords: postfire recovery; burn severity; Scots pine; boreal forests; soil properties; vegetation indices; moisture conditions; edaphic factors

Check for updates

Academic Editors: Wil De Jong and Ioannis K. Kalavrouziotis

Received: 27 February 2026
Revised: 8 April 2026
Accepted: 15 April 2026
Published: 21 April 2026

Copyright: © 2026 by the authors. Licensee MDPI, Basel, Switzerland. This article is an open access article distributed under the terms and conditions of the Creative Commons Attribution (CC BY) license.

1. Introduction

Recent studies have demonstrated that postfire forest recovery is strongly controlled by burn severity, moisture availability, and site-specific environmental conditions. In

particular, the regeneration of Scots pine (*Pinus sylvestris*) depends on the preservation of seed sources and soil properties [1]. Climate–fire interactions and increasing aridity further complicate recovery trajectories in boreal and semiarid regions [2,3].

Recent global assessments indicate a significant increase in wildfire activity under ongoing climate change. According to the IPCC Sixth Assessment Report [4] and recent global fire analyses, the frequency of extreme fire weather conditions has increased in many regions, including boreal and temperate zones. In particular, the length of the fire season has increased by approximately 20–30% globally since the 1980s, while the area affected by high-severity fires has expanded in both North America and Eurasia.

Recent studies have also demonstrated that burn severity and the proportion of large, high-severity fires are increasing, particularly in regions experiencing prolonged droughts and elevated temperatures [5,6]. These trends are associated with increasing fuel dryness and the increasing occurrence of compound climate extremes, factors that increase the spread and severity of fires.

As a result, contemporary fire regimes are undergoing substantial shifts, leading not only to more frequent disturbances but also to more pronounced impacts on forest structure, ecosystem functioning, and postfire recovery trajectories [7,8].

Wildfires are considered among the dominant disturbance factors in forest ecosystems and shape their spatial structure, biogeochemical cycles, and successional dynamics [9,10]. Under ongoing climate change, fires are increasingly leading not only to vegetation renewal but also to shifts in successional trajectories, including delayed recovery of the tree layer and transitions of forests toward alternative stable states [11,12].

Postfire succession is a complex and nonlinear process governed by climatic conditions, topography, soil properties, stand structure, the availability of seed sources, and fire characteristics [13,14]. Despite an extensive body of literature, the role of fire intensity in determining the direction and rate of ecosystem recovery remains a subject of debate. Several studies have shown that high-intensity fires result in a pronounced reduction in tree regeneration and an increased likelihood of forests transitioning to nonforest states [12,15], whereas other research has demonstrated the potential for successful recovery even after high-intensity fires when favourable climatic conditions and sufficient seed availability are present [8,10].

In this context, postfire ecosystem dynamics can be conceptualized within a "dose–response" framework, where fire intensity represents the disturbance "dose" and vegetation recovery reflects the ecological "response". Such an approach allows the integration of burn severity and time since fire into a unified analytical model, enabling the interpretation of recovery trajectories as time-dependent processes rather than static states. Within this framework, different fire intensities are expected to produce distinct recovery pathways characterized by varying rates of regeneration, structural development, and species composition [16].

Additional uncertainty in the interpretation of results arises from methodological differences among studies, including the use of different indicators of fire intensity, varying durations of postfire observation periods, and limited comparability of regional environmental conditions [17,18]. As a result, there is still no consensus on universal patterns of forest ecosystem recovery as a function of fire intensity, particularly in ecotonal and climatically vulnerable regions.

The selection of the Kostanay Region as the study area is determined by several factors. The region is located within a transition zone between forest–steppe and boreal ecosystems and is characterized by high sensitivity to climatic variability and fire disturbances. Under such ecotonal conditions, postfire recovery processes exhibit substantial

variability and may follow different trajectories depending on disturbance intensity and local environmental conditions [19,20].

In addition, the Kostanay Region is an area with elevated fire risk, where recent years have been marked by an increase in both the frequency and extent of forest fires, which is consistent with broader trends of intensifying fire activity in boreal regions [21]. The presence of extensive burned areas with varying degrees of vegetation damage provides favourable conditions for analyzing the effects of fire intensity on recovery processes.

Forest management in the Kostanay Region is aimed at reducing fire hazards and maintaining the stability of forest ecosystems under conditions of frequent fire disturbances. In stands of Scots pine (*Pinus sylvestris L.*), which predominantly occurs on sandy soils, sanitary and selective logging practices are applied to reduce fuel loads and increase stand resistance to fire, in accordance with current forestry regulations of the Republic of Kazakhstan (Sanitary Rules in Forests of the Republic of Kazakhstan, 2015 [22].

In addition, thinning operations are widely implemented to regulate stand density and species composition, thereby enhancing resistance to adverse factors, including fire.

Birch and aspen stands (*Betula* spp., *Populus tremula* L.) are characterized by a high capacity for vegetative regeneration, which is taken into account in forest management planning. In these forest types, management practices are oriented toward utilizing their natural regenerative potential and maintaining stand stability following fire disturbances [23].

Notably, the number of studies in northern Kazakhstan that combine field observations with long-term satellite data remains limited. Moreover, recent studies have demonstrated the high effectiveness of integrating remote sensing and ground-based data for assessing postfire forest dynamics. In this context, the selection of the Kostanay Region helps to address this gap and provides results that are relevant for similar environmental conditions [24].

Contemporary remote sensing approaches based on Landsat data and spectral indices (NBR, dNBR, NDVI, and NDMI) are widely used to assess fire damage and monitor vegetation recovery [17–20]. However, without field-based validation, such assessments may lead to biased estimates of successional rates and directions, especially in heterogeneous and mosaic landscapes [21].

Gitas et al. [22] and Chu and Guo [23] were among the first to provide comprehensive systematic reviews of postfire monitoring methods and techniques. Banskota et al. [24], Zhu [25], Tewkesbury et al. [26], and Hirschmugl et al. [27] subsequently presented extensive syntheses and critical evaluations of algorithms developed for the analysis of multitemporal satellite imagery, including their applications in monitoring wildfire-affected areas. Bartels et al. [28] conducted a quantitative meta-analysis to estimate vegetation recovery times following wildfires, whereas Cohen et al. [29] performed a comparative assessment of the principal algorithms used to map the full spectrum of forest disturbance magnitudes.

In the forest-steppe and boreal regions of arid zones, the interactions among climatic constraints, atmospheric moisture deficits, and tree species composition strongly influence fire regimes and forest ecosystem recovery trajectories. Previous studies have shown that droughts and wildfires act as key drivers of forest dynamics, whereas the dominance of specific tree species can affect both fire intensity and postfire recovery processes [30,31].

In accordance with the national fire hazard map of the Republic of Kazakhstan, the Kostanay region is classified as a high-fire-risk zone. During the period of 2018–2023, the cumulative burned area in the region exceeded 2.02 million ha [32]. However, studies that integrate detailed field observations with long-term satellite time series data to quantitatively assess postfire forest recovery across a gradient of burn severity are lacking for northern Kazakhstan.

To address these limitations, this study adopts an analytical framework that combines burn severity classification with the explicit consideration of time since fire, allowing postfire recovery to be interpreted along a gradient of disturbance intensity and recovery stage. Although long-term continuous time series are not available for all the sites, the inclusion of plots affected by fires of different ages enables a space-for-time substitution approach to approximate recovery trajectories.

According to national statistics, the total burned area in the Kostanay region exceeded 2.02 million hectares during the period of 2018–2023. Notably, this value includes not only forest fires but also burned steppe and agricultural lands. Compared with long-term average values for northern Kazakhstan, recent years have shown a substantial increase in burned area, indicating an intensification of fire activity in the region [5,33,34].

The aim of this study was to quantitatively assess the effects of burn severity on the recovery of forest structure and productivity in the Kostanay region through the integration of field-based observations and long-term Landsat satellite time series.

Under conditions of high pyrogenic pressure on forest ecosystems in northern Kazakhstan, the factors controlling postfire vegetation recovery trajectories, as well as the degree of agreement between field-based and remotely sensed assessments of these processes, remain insufficiently understood.

Therefore, the main research questions of this study are as follows:

(1) How do postfire vegetation structure and regeneration indicators (including the density of viable saplings, proportion of damaged individuals, and stand characteristics) vary across different burn severity classes?
(2) How do satellite-derived spectral indices (NDVI, NDMI, and NBR) respond to variations in postfire vegetation conditions, and how consistently do they reflect field-based indicators of recovery?
(3) To what extent do differences in burn severity explain the observed spatial variability in postfire forest recovery under heterogeneous environmental conditions?

The central hypothesis of this study is that postfire recovery trajectories of forest ecosystems follow a "dose–response" pattern, where fire intensity acts as a key controlling factor determining the direction and rate of vegetation recovery over time. In this framework, low- and moderate-intensity fires are expected to create more favourable conditions for regeneration than high-intensity fires are because of the partial preservation of stand structure, viable seed sources, and more favourable soil and moisture conditions. Accordingly, different fire intensity classes are associated with distinct recovery pathways and successional states.

2. Materials and Methods

2.1. Study Area

The study area encompasses the forested landscapes of the Kostanay Region in northern Kazakhstan. The spatial distributions of the forest types and dominant tree species are shown in Figure 1.

Forests of the Kostanay region are represented primarily by Scots pine (*Pinus sylvestris* L.) stands and mixed birch–aspen forests (*birch* (*Betula* spp.) and aspen (*Populus tremula* L.)), whose ecological characteristics and responses to fire differ substantially. Pine stands, which typically develop on sandy substrates, are characterized by greater flammability because of the accumulation of dry litter and coarse woody debris, and their regeneration depends largely on seed availability and postfire microsite conditions.

In contrast, birch–aspen forests occur on relatively more fertile sites and exhibit lower flammability along with a high capacity for vegetative regeneration, which leads to rapid recovery after fire disturbances. These differences in fuel structure and regeneration

strategies make the dominant forest types of the region particularly suitable for analyzing postfire recovery processes across a gradient of burn severity.

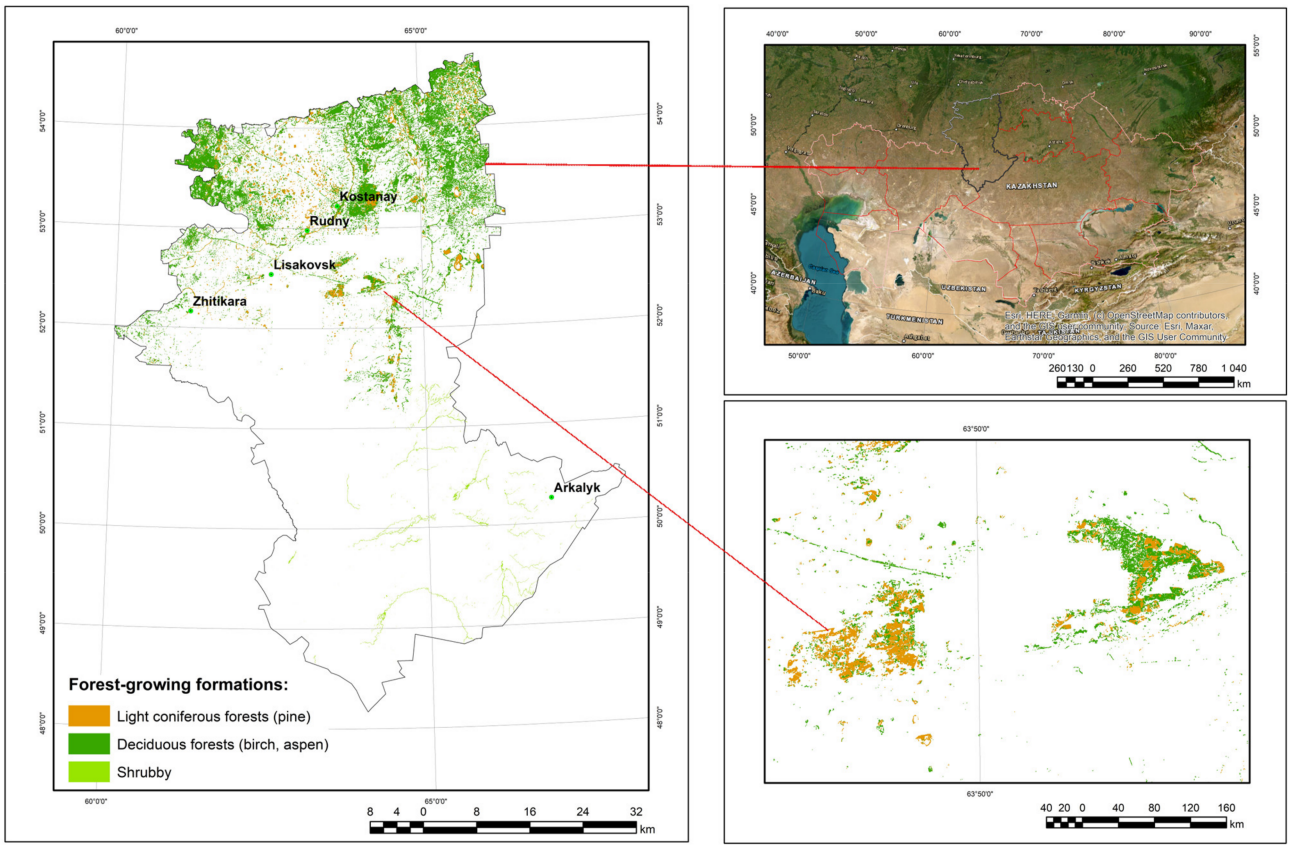


Figure 1. Spatial distribution of the dominant forest-forming species in the Kostanay Region. Source: Created by the authors via public-domain Landsat 8 OLI surface reflectance imagery (USGS/NASA) and field survey data collected in 2023.

Birch (*Betula* spp.) and aspen (*Populus tremula* L.) stands are predominantly distributed along the lower sections of sandy ridge slopes and frequently occur in proxies to saline lake shorelines. Shrub willows (*Salix* spp.) and honeysuckle (*Lo-nicera* spp.) are commonly found along riverbanks and lake margins, whereas rosehip (*Rosa canina* L.) and meadowsweet (*Filipendula ulmaria* (L.) *Maxim.*) are characterized by foot-hill zones and gentle slopes. Clearings and forest glades are dominated by sandy steppe and feathergrass (*Stipa* spp.) communities, whereas narrow belts of meadow–saline vegetation are typical along forest edges.

A distinctive structural feature of forests in northern Kazakhstan is the predominance of small-diameter trees. During wildfire events, these thin-stemmed individuals are among the first to be affected, leading to substantial tree mortality and stand degradation. When the forest stands were considered assemblages of individual trees within the sampling plots, the mean stem diameter ranged from 14 to 28 cm. Consequently, the proportion of small-diameter trees in the studied forests is approximately twice that observed in typical forest stands across northern Kazakhstan.

The predominance of small-diameter trees is determined by the regional landscape structure, the confinement of forests to sandy substrates with low soil water-holding capacity, and recurrent wildfires and anthropogenic disturbances. Such a stand structure increases forest vulnerability to high-intensity fires because of the low fire resistance and limited pyrogenic tolerance of thin-stemmed trees.

The study area is located in northern Kazakhstan and lies within a sharply continental climate zone characterized by limited atmospheric precipitation. These conditions create unfavourable environments for postfire forest recovery on sandy substrates.

The study area is located in northern Kazakhstan and lies within a strongly continental climate zone characterized by limited precipitation. These conditions create an unfavourable environment for postfire forest recovery on sandy substrates.

The climate of the Kostanay Region is strongly continental, with cold winters and hot, dry summers. The mean annual air temperature ranges from approximately +1.5 to +2.5 °C, with mean January temperatures of −17 to −19 °C and mean July temperatures of +19 to +22 °C. Absolute minimum temperatures may decrease to −40 °C, whereas maximum summer temperatures can reach +38 to +40 °C.

The annual precipitation ranges from 250 to 350 mm, with approximately 60–70% occurring during the warm season (April–September), peaking in June–July and reaching a minimum during the winter months. This results in pronounced seasonality of moisture availability. Such climatic conditions contribute to elevated fire risk and strongly influence postfire forest ecosystem recovery processes [35].

2.2. Data Collection

The fire-prone season in the region is characterized by two distinct peaks—spring–summer and summer–autumn—which determine the temporal framework of the field surveys. Field investigations were conducted during the summers of 2023–2025 and included both ground-based and geospatial observations. Unburned reference sites were used as baseline conditions for comparison with areas affected by fires of varying intensity, following standard approaches in disturbance ecology studies [36,37].

The establishment of the sampling points followed the Forest Management Instruction (2012) [35] and was supported by the integration of the Landsat 8 OLI, Sentinel-2 MSI, and NASA Goddard Space Flight Center datasets in combination with the orman.gharysh.kz geospatial platform (Figure 2). Field surveys were conducted during the same growing seasons as the postfire satellite imagery used in the analysis, ensuring comparability between ground-based and remotely sensed assessments. The use of remote sensing data at the sampling design stage enabled reproducibility of the spatial layout of the sampling plots [38,39].

The sampling plots were established in homogeneous forestland sites located at least 30 m from adjacent land use categories. Plots were positioned within stands affected by fires of varying intensity, as well as in clear-cut and burned areas, and in control plots that had not been exposed to fire.

The spatial distribution of the sampling plots ensured the representation of all the burn severity classes while maintaining the comparability of the background environmental conditions, with multiple plots established within each class [38,39].

The sampling design included both pine-dominated stands and mixed stands, allowing coverage of the principal types of postfire forest landscapes in the Kostanay region. Of the 22 sampling plots, 16 were established in pine-dominated stands, whereas 6 plots represented mixed or deciduous (birch–aspen) forests.

The control plots included forest areas that had not been affected by fire for an extended period, as well as sites representing postlogging stands and areas that had regenerated following previous fire events. Comparability between control and fire-affected plots was ensured by maintaining similarities in site conditions, topography, soil characteristics, stand composition, and stand age and—where applicable—by accounting for the time elapsed since logging or burning.

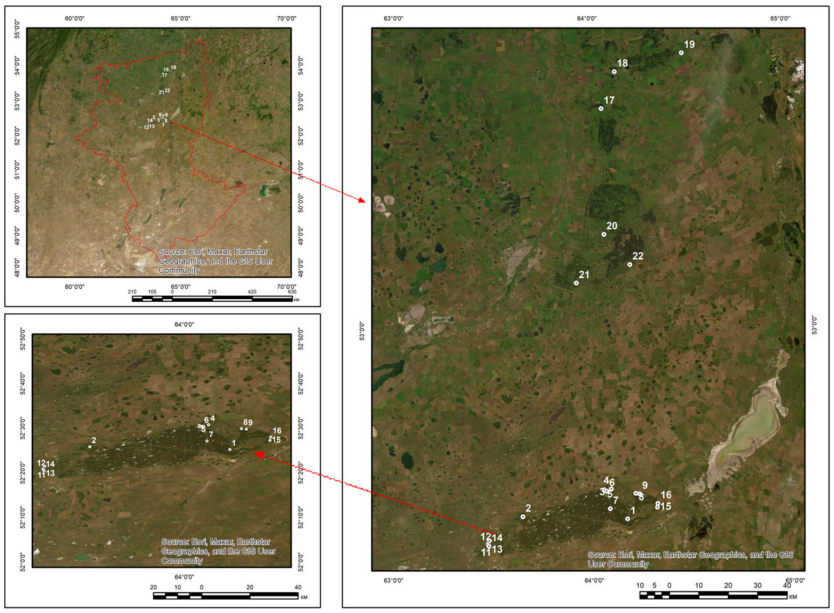


Figure 2. Spatial distribution of the sampling plots within the study region. Source: Created by the authors via public-domain Landsat 8 OLI imagery (USGS/NASA) and field survey data.

The establishment and description of the sampling plots (0.20–0.25 ha in area) were conducted in accordance with the standard methods proposed by V. N. Sukachev and S. V. Zonn [39]. The classification of fire-affected sites followed the guidelines developed by I. S. Melekhov [40].

Thus, the identification of fire type and intensity under field conditions is based on standardized indicators of stand damage that are widely used in forest fire research [40,41]. The size of each sampling plot was selected to ensure that at least 200 trees of the dominant forest-forming species were represented within its boundaries.

Permanent (fixed) sample plots were not established because the study was designed as a spatially distributed assessment of postfire conditions across multiple sites differing in fire intensity and time since disturbance. The use of temporary sampling plots allowed coverage of a broader range of environmental conditions and fire histories within the study region.

The inclusion of at least 200 trees within each sampling plot ensured a sufficient sample size for reliable estimation of stand structure parameters and reduced the influence of individual tree variability. This threshold is consistent with standard forest inventory practices and provides a statistically robust characterization of stand conditions at the plot level.

The selection of the sampling plots followed a stratified design rather than a purely random approach. Plots were allocated across predefined burn severity classes (reference, low–moderate, and high) to ensure balanced representation of postfire conditions. Within each class, sites were selected to maintain comparable environmental characteristics (soil type, relief, and forest composition).

The spatial distribution of the sampling plots was designed to ensure coverage of the study area while minimizing spatial autocorrelation; the distance between plots typically exceeded 500–1000 m.

The initial classification of burn severity was based on standardized field-based indicators of forest stand conditions, including crown damage, stem char characteristics, and the degree of ground vegetation and litter consumption, prior to subsequent validation using dNBR derived from satellite data.

The burn severity classes were determined using a combination of remote sensing indicators (primarily NBR differencing from Landsat data) and field-based observations of burn severity (including canopy damage, soil surface alteration, and vegetation mortality). This integrated approach ensured consistent classification of burn severity across all the sampling plots.

On the basis of the requirements for plot representativeness, comparability of background environmental conditions, and adequate statistical replication, a total of 22 sampling plots were established and distributed across burn severity classes (low, moderate, and high). Each class was represented by multiple plots (at least 5–7), allowing for statistically robust comparisons. On average, approximately 80 measurement points were collected within each plot.

The established sampling plots represent the main types of forest ecosystems within the study area, including pine-dominated stands and mixed birch–aspen forests distributed across the Kostanay region. The selection of plots was designed to capture the spatial variability of postfire conditions across different fire intensity classes while maintaining comparable site characteristics.

Statistical representativeness was ensured through the balanced distribution of sampling plots among fire intensity classes and the inclusion of multiple plots within each class (at least 5–7 plots per group). This design allowed for robust comparative analysis while minimizing the influence of site-specific anomalies.

The experimental design of the study had a hierarchical structure. The sampling plot ($n = 22$) was considered the primary experimental unit, whereas individual measurement points within each plot (approximately 80 per plot) were used as subsamples and were not treated as independent observations.

All the variables were aggregated at the level of the sampling plot prior to statistical analysis. Accordingly, statistical analysis was conducted at the plot level, which ensured the avoidance of pseudoreplication and allowed for valid comparisons among plots [38,42].

The sampling plots were grouped according to burn severity classes (reference conditions, low–moderate, and high), and all the statistical comparisons were performed among these groups.

Unburned control plots were used as reference conditions and were included in the analysis as a separate group (reference). A total of 13 control plots were identified, which were comparable to the studied sites in terms of species composition, soil conditions, and stand structure.

Control plots were considered part of the overall environmental gradient and were used for statistical comparison with plots affected by different levels of burn severity, which is consistent with established approaches in ecological studies [43,44].

The spatial distributions of the sampling plots and their relationships with the fire-affected areas are shown in Figure 2.

The age of the dominant tree component was determined by counting annual rings in increment cores collected at the root collar or from stumps of felled trees, following standard dendrochronological approaches [45]. Stem diameter was measured at a height of 1.3 m, and tree height was determined using remote measuring instruments in accordance with standard forest inventory methods [46]. The physical properties of wood (moisture content and temperature) and soil parameters (bulk density, moisture content, temperature, pH, and humus content) were determined using standard field and laboratory methods.

Soil samples were collected from the upper organomineral horizon at a depth of 0–10 cm, which is the layer most sensitive to fire effects. In each sampling plot, 5–7 sampling points were established and evenly distributed across the area. These subsamples were

combined into a single composite sample to provide a representative characterization of soil conditions at the plot level.

To evaluate the success of natural postfire forest regeneration, an integrated set of indicators, including parameters of tree regeneration, stand retention, and soil conditions, was employed. Soil pH, humus content, soil bulk density, and soil moisture are considered interrelated environmental characteristics that collectively shape conditions for postfire forest recovery [47]. Soil samples for these analyses were collected from the upper organomineral horizon (0–10 cm depth), with 5–7 subsamples taken within each sampling plot and combined into a composite sample. These variables were subsequently used in the analysis to interpret differences in postfire regeneration success among the sites (Table 1).

Table 1. Field-based indicators and methods used in the study.

Indicator	Description	Measurement Method
Density of viable saplings	Number of healthy regenerating individuals per unit area	Field inventory within subplots following Buzykin and Pobedinsky [44]
Density of damaged saplings	Number of saplings with visible fire damage	Field inventory and classification by physiological condition
Proportion of surviving trees	Percentage of trees remaining after fire	Visual assessment of stand condition
Stand density (canopy closure)	Degree of canopy cover (0–1 scale)	Visual classification based on standard forestry methods
Tree diameter (DBH)	Stem diameter at 1.3 m height	Measured using a calliper
Tree height	Height of trees	Measured using a laser rangefinder
Wood moisture content	Moisture content of wood	Measured using a wood moisture meter (DMM-001)
Soil moisture	Soil water content	Measured using TRS-II digital soil moisture meter
Soil temperature	Soil thermal conditions	Measured using digital sensors
Soil bulk density	Soil compaction and structure	Measured using a TYD-2 penetrometer
Soil pH	Soil acidity	Measured using SDT-60 pH meter
Humus content	Organic matter content in soil	Determined according to GOST 23740-2016

The type, form, and intensity of fire were identified on the basis of standardized indicators of forest stand conditions, including the degree of crown damage and dieback; the height of tree trunks; the extent of bark and root collar charring; and the level of ground vegetation, old stump, and downed deadwood combustion.

Field-based fire indicators have been used to validate satellite-derived estimates of burn severity [48,49]. The resulting remote sensing metrics of burn severity (NBR and dNBR) were subsequently applied to classify the sampling plots and to support further statistical analyses [36,37,49]. Their effectiveness has been confirmed in recent studies integrating multisensor data, including Landsat, Sentinel-2, and LiDAR observations [20,50]. These approaches enable consistent monitoring of vegetation dynamics and structural changes following wildfire disturbances.

The ages of the fire events and interfire intervals were determined via cross-sections from tree trunks bearing fire scars, as well as from stumps of felled dead trees. The time elapsed since the fire was further verified by analyzing the age structure and conditions of the regenerating saplings.

At each sampling point, saplings and naturally regenerated individuals were inventoried within designated subplots, where the number of surviving and newly established postfire saplings was recorded following the methodology proposed by A. I. Buzykin and A. V. Pobedinsky [51].

Sapling inventories were constructed within fixed-area subplots that were systematically distributed within each sampling plot.

The stand type, species composition, and stand density were determined in accordance with the classification system of M. M. Orlov. Stand age, mean height, and growing stock per hectare and per compartment prior to fire events were established on the basis of data collected at the sampling points.

Saplings were classified as healthy or damaged according to their physiological condition. In accordance with standard forest regeneration classifications, the saplings were further grouped into three height classes: small (≤0.5 m), medium (0.51–1.5 m), and tall (>1.5 m).

Crown closure was classified on an interval scale: 0.3–0.5—open canopy, 0.5–0.7—moderately closed canopy, and >0.7—closed canopy.

Saplings were classified as viable (healthy) when crown integrity was maintained and no significant pyrogenic damage was observed. Damaged saplings included individuals exhibiting partial crown mortality, root collar burns, and pronounced signs of growth suppression.

Field permits and site access: Field observations and sample collection were conducted exclusively on publicly accessible forestland; therefore, no special permits were required for this research. The study did not involve activities within protected areas, endangered species, or privately owned territories. All fieldwork was carried out in accordance with the Forest Management Instruction of the Republic of Kazakhstan (2012) [52].

The spatial context of the study area and the distribution of forest fires used in the design of the sampling network are illustrated by the burn scar map of the Kostanay Region for the period of 2004–2024 (Figure 3).

In addition to field data, spectral indices, including the normalized burn ratio (NBR), the normalized difference vegetation index (NDVI), and the normalized difference moisture index (NDMI), which provide a quantitative basis for assessing vegetation burn severity and postfire recovery dynamics [53], were used in this study.

These indices were calculated from Landsat 7 ETM+ and Landsat 8 OLI satellite imagery processed for surface reflectance via standard radiometric calibration and atmospheric correction procedures, ensuring temporal consistency and intersensor comparability [53,54]. Landsat 8 OLI data were specifically applied for wildfire analysis [55].

To ensure methodological consistency and reproducibility, satellite data from different sources were used with clearly differentiated roles.

Landsat 7 ETM+ and Landsat 8 OLI surface reflectance data (30 m spatial resolution) were used as the primary dataset for quantitative analysis of postfire vegetation dynamics. These data were used to calculate spectral indices (NDVI, NDMI, and NBR) and to assess vegetation recovery at the level of the sampling plots.

All spectral indices were derived exclusively from Landsat imagery to ensure spatial consistency and comparability across the study area. The spatial resolution of the Landsat data is commensurate with the size of the sampling plots (0.20–0.25 ha), which minimizes the mixed-pixel effect and allows reliable integration with field observations.

MODIS data (MCD64A1 BurnDate product; spatial resolution, 500 m) were used solely for spatiotemporal verification of fire events, including the identification of fire occurrence dates and the delineation of burned areas at the regional scale. MODIS data were not used for quantitative analysis of vegetation recovery because of their coarse spatial resolution.

The integration of the Landsat and MODIS datasets was performed conceptually rather than through direct pixel-level combination. Landsat data provided detailed local-scale information on vegetation dynamics, whereas MODIS data ensured the temporal accuracy and completeness of fire event detection.

Such separation of functions between datasets ensures methodological transparency, reduces scale-related uncertainty, and improves the reproducibility of the analysis.

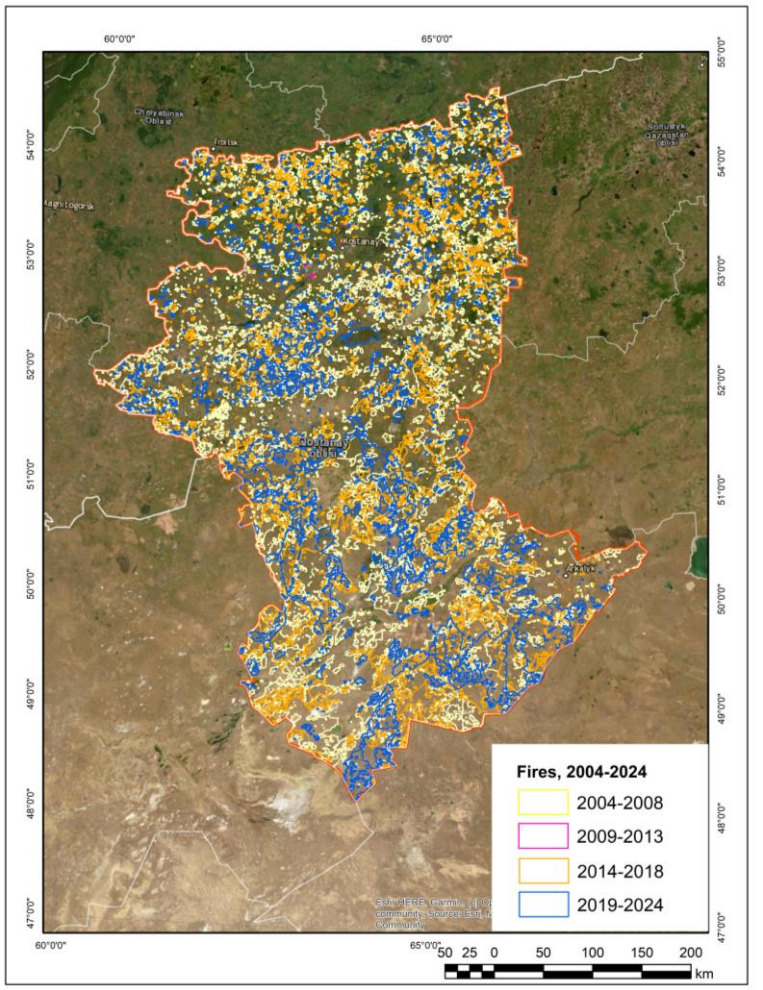


Figure 3. Spatial distribution of forest fire-affected areas in the Kostanay Region (2004–2025). Source: Produced by the authors via Landsat 7–8 imagery (USGS/NASA) and authors' field data analysis.

The normalized difference vegetation index (NDVI) reflects vegetation photosynthetic activity, productivity, and overall biomass accumulation [56,57]. The NDVI values range from −1 to +1, with positive values indicating the presence and physiological conditions of the vegetation. The NDVI was calculated as follows (Equation (1)) [58]:

$$NDVI = (NIR - Red)/(NIR + Red) \quad (1)$$

Elevated NDVI values reflect increased phytomass production and the accumulation of combustible vegetation material, which may influence fire spread patterns and fire impact severity in mature forest stands [58,59]. Remote sensing enables the assessment of the spatial distribution of fuel loads at the landscape scale (Table 2) [58,59].

Table 2. Interpretation of the NDVI values in relation to phytomass and combustible vegetation material.

NDVI Value Range	Interpretation	Vegetation Fuel Characteristics
<0.1	Very low values	Absence of vegetation or extremely sparse cover; minimal amounts of combustible material
0.1–0.3	Low values	Sparse vegetation with low phytomass; limited accumulation of vegetative fuel

Table 2. *Cont.*

NDVI Value Range	Interpretation	Vegetation Fuel Characteristics
0.3–0.5	Moderate values	Well-developed herbaceous–shrub layer or sparse tree cover; moderate accumulation of combustible materials
0.5–0.7	High values	High phytomass, closed forest stands or dense understorey; substantial accumulation of live vegetative fuel
>0.7	Very high values	Dense, well-developed vegetation in mature forest stands; high fuel loads of combustible plant material

The normalized difference moisture index (NDMI) serves as an indicator of the moisture status of the soil–vegetation system and plays a key role in assessing wildfire ignition probability and potential fire intensity [58]. A higher moisture content in both soils and vegetation reduces the likelihood of ignition and attenuates fire intensity once a fire occurs. Consequently, soil water-holding capacity, evaporation rates, and precipitation regimes—parameters that vary with soil type and local hydroclimatic conditions—are important factors controlling spatial and temporal variability in NDMI values. The NDMI was calculated as follows (Equation (2)) [58,60]:

$$\text{NDMI} = (\text{NIR} - \text{SWIR})/(\text{NIR} + \text{SWIR}) \quad (2)$$

In accordance with standard interpretations of NDMI values, the index ranges from −1 to +1, where positive values (>0) indicate the presence of vegetation and soil moisture, whereas negative values correspond to conditions of pronounced atmospheric or soil drought (Table 3) [58,60].

Table 3. Interpretation of NDMI values.

NDMI Value Range	Interpretation	Environmental Condition Characteristics
−1.0 to −0.2	Very low values	Pronounced soil and/or atmospheric drought; absence or severe degradation of vegetation
−0.2 to 0.0	Low values	Dry conditions with sparse or stressed vegetation cover
0.0 to 0.2	Moderate values	Low to moderate moisture availability; sparse or recovering vegetation
0.2 to 0.4	Elevated values	Satisfactory moisture conditions; actively functioning vegetation
>0.4	High values	Well-moisturized soils with dense and healthy vegetation cover

The NDVI and NDMI were calculated as multiyear mean values separately for each sampling plot, using exclusively postfire observations starting from the year of the most recent fire event affecting each site and extending across subsequent growing seasons. The use of multiyear mean NDVI and NDMI values was intended not to characterize short-term recovery dynamics but to identify stable postfire ecosystem conditions following the completion of the initial regeneration phase. This approach has been widely applied in postfire ecosystem studies that analyze remote sensing time series [54,55].

Because the timing of the most recent fire events differed among the sampling plots, the postfire observation periods also varied. To ensure comparability among sites, only postfire observations were included, and multiyear mean values of the NDVI and NDMI were used to represent stabilized postfire conditions rather than specific successional stages.

Accordingly, the analysis focused on comparing relative differences among sites along the burn severity gradient rather than explicitly modelling temporal recovery trajectories.

The time since fire and interfire intervals derived from the tree-ring analysis were used as supporting information for interpreting the results but were not included as independent variables in the statistical models because of the limited sample size and the uneven distribution of plots across fire years [61,62].

To minimize the smoothing effect of early successional stages, only postfire years beginning with the year of the most recent fire affecting each sampling plot were included in the analysis. This approach allows comparisons of sites that differ in the timing of the last fire event on the basis of stabilized recovery characteristics and is commonly applied in analyses of spatial gradients of postfire ecosystem recovery [63,64].

The interpretation of the vegetation and soil moisture conditions was based on the NDMI, which serves as an indicator of the moisture content in live vegetative fuel and plays a key role in postfire processes [58]. For an objective and reproducible assessment of burn severity, the normalized burn ratio (NBR) and its differenced form (dNBR) were used, both of which are widely applied in international fire ecology research [47,48].

The normalized burn ratio (NBR) is a spectral indicator used to delineate burned areas, detect changes in vegetation cover, and assess the degree of disturbance [47]. The normalized burn ratio (NBR) was calculated via the standard formulation as the normalized difference between the near-infrared (NIR) and shortwave infrared (SWIR) reflectances (Equation (3)) [47,48]:

$$NR = \frac{NIR - SWIR}{NIR + SWIR} \quad (3)$$

where *NIR* denotes surface reflectance in the near-infrared spectral band, which is sensitive to vegetation structure and physiological conditions, and *SWIR* denotes surface reflectance in the shortwave infrared band, which is sensitive to vegetation and soil moisture content as well as to thermal effects associated with fire.

NBR values range from −1 to +1, where higher values indicate healthy, undisturbed vegetation, whereas lower or negative values correspond to areas affected by fire or completely devoid of vegetation.

For the quantitative assessment of burn severity, the difference in the normalized burn ratio (dNBR) was calculated as the difference between the prefire and postfire NBR values (Equation (4)) [36]:

$$dNBR = NBRpre - NBRpost \quad (4)$$

where NBR_{pre} denotes the index value calculated for the prefire period and NBR_{post} denotes the value obtained for the postfire period.

The resulting dNBR values were classified via standard burn severity threshold values, providing a unified and reproducible quantitative criterion for assigning sampling plots to burn severity classes and eliminating subjective visual interpretation [36,48].

The burn severity classes were defined as follows [36]:

dNBR < 0.10—no or minimal fire impact;

0.10–0.27—low burn severity;

0.27–0.44—moderate burn severity;

0.44—high burn severity.

The ecological interpretation of the defined burn severity classes is presented in Table 4 [36].

Table 4. Classification of burn severity on the basis of *dNBR* values.

dNBR Range	Burn Severity Class	Impact Characteristics
<0.10	No/minimal impact	Preserved vegetation cover with no pronounced pyrogenic alterations
0.10–0.27	Low	Partial damage to ground vegetation and understorey
0.27–0.44	Moderate	Substantial vegetation damage with partial tree mortality
>0.44	High	Severe burning with mortality of the tree layer and ground vegetation

Each burn severity class was represented by multiple sampling plots, ensuring sample representativeness and enabling robust statistical comparisons among groups.

Thus, the assignment of the sampling plots to burn severity classes was based on clear quantitative criteria rather than subjective visual assessment.

Spatiotemporal verification of fire events

To refine the timing and spatial extent of fire events, the BurnDate layer from the MODIS MCD64A1 product (v6), derived from Terra and Aqua satellite data for the period of 2004–2023, was used [65] (Figure 3). The integration of the MODIS and Landsat data was performed at the level of event correspondence rather than through direct pixel-level spatial alignment, thereby avoiding biases associated with differences in spatial resolution.

2.3. Linking Remote Sensing and Field Data

The comparison of satellite-derived and field-based data enabled a quantitative assessment of the consistency between burn severity indicators and postfire vegetation recovery metrics. Field indicators of fire effects, including the char height on tree trunks, degree of crown damage, and degree of ground vegetation layer combustion, were used to validate remote sensing-based estimates of burn severity derived from dNBR values [47,48].

The quantitative agreement between the field and remote sensing indicators was further evaluated via correlation analysis, allowing assessment of the robustness of the relationships among burn severity metrics, sapling regeneration characteristics, and spectral indices (NDVI, NDMI, and NBR).

The spatial resolution of satellite data was explicitly considered during result interpretation by aggregating indicators at the sampling-plot level. Because the plot dimensions exceeded the spatial resolution of the Landsat sensors, the influence of mixed pixels was reduced, thereby increasing the reliability of the analytical results [47,48].

2.4. Statistical Analysis

Statistical analysis was designed to assess differences among burn severity classes, which were treated as the main explanatory factor. The burn severity class (reference, low–moderate, or high) was considered a fixed effect.

All analyses were conducted at the level of the sampling plots, which represented independent experimental units (n = 22). Variables derived from measurements within plots were aggregated prior to analysis.

Given the limited sample size and the study design, random effects were not included in the statistical models.

Temporal variables (time since fire and interfire intervals) were not incorporated as predictors but were considered qualitatively during the interpretation of the results.

Soil properties (humus content, soil pH, moisture, and bulk density) were analyzed as explanatory variables and were primarily used to interpret observed differences in postfire recovery among plots rather than as predictors in a unified multivariate model.

Differences among the sites affected by varying burn severity were analyzed via descriptive and inferential statistical methods. For each variable examined—including the densities of viable and damaged saplings, spectral indices (NDVI, NDMI, and NBR), and soil properties—mean values and standard deviations were calculated.

Prior to applying the parametric tests, the statistical assumptions of normality (Shapiro–Wilk test) and homogeneity of variance (Levene's test) were assessed [66,67]. Depending on whether these assumptions were met, differences among burn severity classes were evaluated via one-way analysis of variance (ANOVA) or its nonparametric counterpart, the Kruskal–Wallis test [68]. Post hoc comparisons were performed to identify pairwise differences between groups [69].

All the statistical analyses were performed in R (version X.X.X; R Core Team, 2023) using standard packages, including "stats" for analysis of variance and "corrplot" for visualization of correlation matrices. When multiple pairwise comparisons were conducted, p values were adjusted using the Tukey honestly significant difference (HSD) procedure to control for Type I error.

Relationships between field-based recovery indicators and remote sensing spectral indices (NDVI, NDMI, and NBR) were assessed via Spearman's rank correlation analysis, which is robust to deviations from normality [63]. This approach is widely applied in contemporary postfire ecosystem studies based on Landsat time series data [61,62].

The results of the statistical analyses were visualized via boxplots and correlation matrices. Statistical significance was set at $p < 0.05$. All the statistical analyses were performed via the R statistical computing environment [70].

Given the limited number of sampling plots and the heterogeneity in the timing of plot establishment, the statistical analysis focused on comparative and interpretative assessments of differences among burn severity classes rather than on the development of predictive models. Temporal factors (time since fire and interfire intervals) were considered during interpretation of the results but were not explicitly included as predictors in the statistical models.

The relationships between the variables analyzed and the statistical methods applied are summarized in Table 5.

Table 5. Statistical methods used for data analysis.

Variable	Data Type	Assumptions Tested	Comparison Among Burn Severity Classes	Additional Analysis
Density of viable saplings	Quantitative	Shapiro–Wilk, Levene	ANOVA/Kruskal–Wallis	Tukey post hoc test
Density of damaged saplings	Quantitative	Shapiro–Wilk, Levene	ANOVA/Kruskal–Wallis	Tukey post hoc test
NDVI	Quantitative	Shapiro–Wilk, Levene	ANOVA/Kruskal–Wallis	Spearman correlation
NDMI	Quantitative	Shapiro–Wilk, Levene	ANOVA/Kruskal–Wallis	Spearman correlation
NBR	Quantitative	Shapiro–Wilk, Levene	ANOVA/Kruskal–Wallis	Spearman correlation
Soil properties	Quantitative	Shapiro–Wilk, Levene	ANOVA/Kruskal–Wallis	Spearman correlation

Note: The choice between parametric and nonparametric methods was determined based on the results of normality (Shapiro–Wilk test) and homogeneity of variance (Levene's test).

Table 5 summarizes the statistical methods used in the analysis and does not present empirical results. The detailed results are provided separately in the Appendix A (Tables A1–A3).

All the statistical analyses were conducted using aggregated values at the level of the sampling plots, with each sampling plot treated as an independent observation. Measurements collected within each plot were not considered independent replicates.

2.5. Integration of Soil and Biotic Indicators

The soil pH, humus content, soil bulk density, and soil moisture were not considered in isolation but rather as interrelated complexes of edaphic factors that jointly shape conditions for postfire forest ecosystem recovery. These parameters regulate nutrient availability, the soil water regime, microbial activity, and seed germination conditions, thereby directly influencing the survival and growth rates of regenerated trees following fire events [45,71,72].

The humus content is used as an integrated indicator of soil fertility and water-holding capacity, which is particularly critical under the sandy and loamy-sandy soil conditions characteristic of northern Kazakhstan [45,72]. Soil pH is considered a modifying factor affecting nutrient availability and the intensity of microbiological processes that are sensitive to the thermal effects of fire [45]. Soil bulk density and moisture reflect the degree of postfire degradation of the soil structure and the suitability of rooting conditions for regenerating saplings [72–74].

The above soil characteristics were subsequently analyzed jointly with biotic indicators (densities of viable and damaged saplings and stand retention) and satellite-derived indices (NDVI, NDMI, and NBR) to interpret differences in postfire recovery success among sites subjected to varying levels of burn severity. This integrative approach allows soil parameters to be treated as modifying factors of recovery trajectories rather than as independent descriptive variables.

Measurements of the soil parameters were conducted via calibrated instruments, and repeated measurements were performed on a subset of the sampling plots to assess the data reproducibility. The measurement uncertainties for soil pH and moisture did not exceed the limits specified by instrument technical specifications and standardized methodological guidelines, ensuring the comparability of indicators across plots and the validity of subsequent analyses.

Within the framework of this study, postfire recovery is interpreted using a conceptual dose–response model, in which burn severity (assessed using dNBR) is treated as the disturbance factor (dose), while forest recovery indicators—such as sapling density, the proportion of surviving trees, and spectral indices (NDVI, NDMI, and NBR)—represent the ecosystem response.

The temporal dimension of recovery is accounted for through the parameter time since the fire, which is determined on the basis of field dendrochronological data and satellite observations. Thus, each sampling plot can be interpreted as a point within the "burn severity–time since fire" space, allowing the set of plots to be considered an approximation of a family of postfire recovery trajectories.

Given the multifactorial nature of postfire forest ecosystem recovery and the need to simultaneously account for soil, biotic, and remote sensing indicators, an integrative analytical framework was applied in this study. To clearly illustrate the data-processing logic, analytical workflow, and relationships among the variables considered, a conceptual framework was developed and is presented in Figure 4.

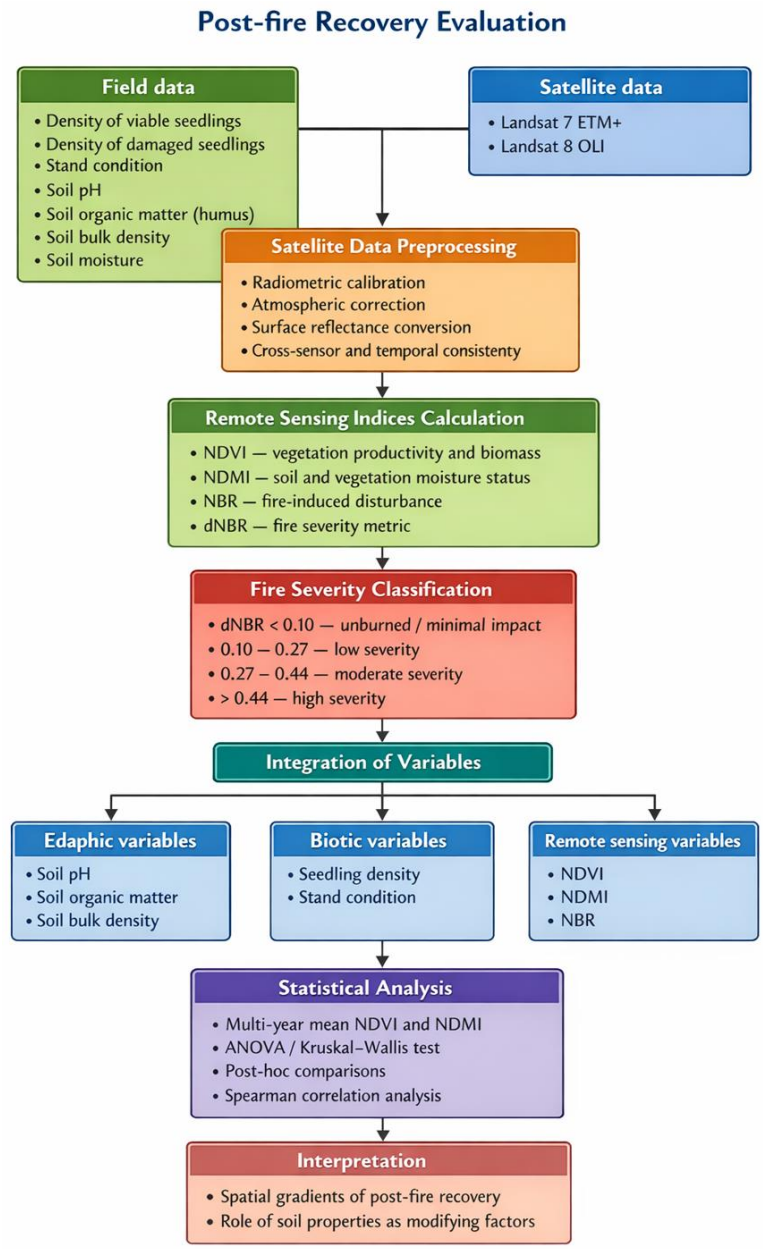


Figure 4. Conceptual framework of the study methodology.

This conceptual framework summarizes the integrated methodological approach used to assess postfire forest ecosystem recovery. It illustrates the integration of field-based soil and biotic measurements with satellite-derived remote sensing indices (NDVI, NDMI, NBR, and dNBR), the sequence of data preprocessing and analysis steps, the classification of burn severity, and the evaluation of postfire recovery trajectories while accounting for edaphic controls.

3. Results

Field investigations were conducted between 2023 and 2025 across 22 sampling plots, including reference (unburned) sites and areas differing in fire type and time elapsed since disturbance. To ensure comparability of the results, all the plots were grouped according to fire type (crown and surface fires) and burn severity classes (reference; low–moderate; high), which were defined on the basis of the NBR and dNBR indices calculated from the Landsat imagery. This classification served as a unified analytical framework for integrating and comparing field-based, soil, and satellite-derived indicators of postfire ecosystem recovery.

The obtained results should be interpreted not as a static comparison among sites but as a representation of different stages of postfire recovery shaped by varying levels of burn severity and time since fire. Thus, the observed differences among sites represent a set of recovery trajectories corresponding to different combinations of the factors "burn severity–time since fire".

The spatial distributions of the spectral indices NDVI, NDMI, and NBR reveal pronounced heterogeneity in vegetation conditions and moisture availability within the study area (Figure 5). Sites characterized by reduced NDVI and NDMI values are associated with areas subjected to severe pyrogenic impact and substantial vegetation loss, whereas elevated spectral index values are typical of reference sites and areas undergoing partial recovery.

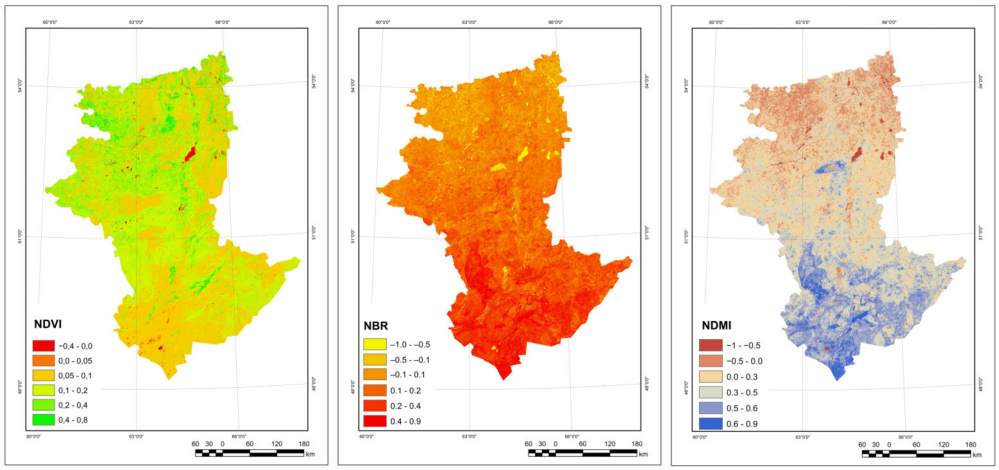


Figure 5. Spatial distributions of the NDVI, NBR, and NDMI across the study area derived from Landsat imagery.

The observed spatial mosaic of spectral indices reflects heterogeneity in pyrogenic impact and differences in vegetation recovery conditions. To quantitatively formalize these differences and standardize subsequent comparisons, the sampling plots were classified by burn severity via the dNBR index (Figure 6).

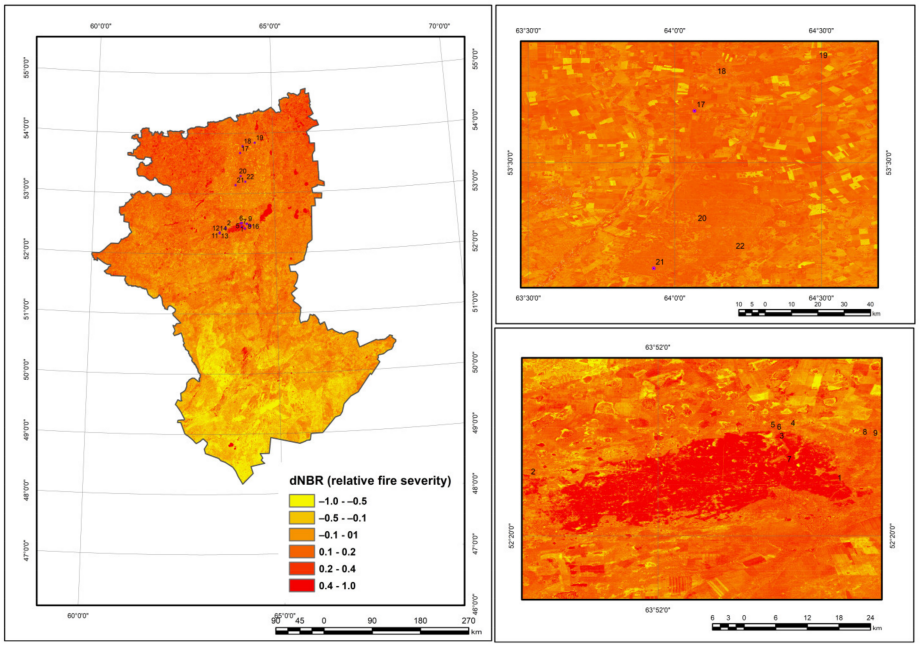


Figure 6. Classification of burn severity on the basis of the dNBR index calculated for the year of the most recent fire at each sampling plot.

On the basis of widely accepted threshold values, the sampling plots were classified into reference (dNBR < 0.10), low–moderate burn severity (0.10–0.44), and high burn severity (dNBR $\geq$ 0.44) classes [36]. This classification was used as a unified analytical framework for comparing field-based, soil, and satellite-derived indicators of postfire ecosystem recovery.

The burn severity classes derived from the dNBR are clearly illustrated by the characteristics of the individual sampling plots. Plots 1, 2, and 5, assigned to the high-burn severity class and affected by recent fires of different types, presented the most pronounced stand structure disturbance and reduced vegetation and moisture index values. In contrast, plots 17 and 19, representing reference or weakly disturbed conditions, are characterized by a preserved canopy structure, higher spectral index values, and more favourable moisture conditions. These examples demonstrate that dNBR-based classification provides a consistent and robust framework for integrating field, soil, and remote sensing indicators of postfire recovery.

To improve clarity and avoid excessive grouping of variables, the previously combined results have been reorganized and are now presented in separate tables in the Appendix A: stand structure and fire regime (Table A1), regeneration characteristics and species composition (Table A2), and soil properties and spectral indices (Table A3).

The analyzed indicators exhibited substantial variability across the sampling plots and burn severity classes (Tables A1–A3). This variability reflects differences in postfire conditions, time since disturbance, and site-specific environmental factors. Overall, the observed patterns indicate that both fire intensity and local environmental conditions play key roles in shaping postfire forest recovery.

The field-based, soil, and satellite-derived indicators presented in Table 2 exhibit high interplot variability, reflecting differences in fire type and burn severity, time elapsed since pyrogenic disturbance, and local site conditions. In particular, plots subjected to high burn severity show a pronounced reduction in the density of healthy saplings and the proportion of surviving trees, whereas reference and weakly disturbed plots are characterized by higher NDVI and NDMI values and greater canopy closure. Such data heterogeneity precludes reliance on descriptive comparisons alone and necessitates the application of formal statistical methods to identify robust differences among fire severity groups. Accordingly, prior to conducting groupwise comparative analyses, statistical assumptions were tested for all quantitative variables, including the normality of distributions and the homogeneity of variances, following standard procedures for the analysis of highly variable ecological data [75,76]. The results of assumption testing and the rationale for the selection of statistical tests are presented in Table 6.

Table 6. Statistical assumptions and analytical tests were applied.

Variable	Shapiro–Wilk (p)	Levene's Test (p)	Applied Test	Overall p Value
Healthy saplings (thousand stems ha^{-1}).	7.62×10^{-6}	0.00529	Kruskal–Wallis	0.026
Damaged saplings (thousand stems ha^{-1}).	8.69×10^{-9}	0.0167	Kruskal–Wallis	0.000229
Surviving trees (%)	5.47×10^{-7}	0.0494	Kruskal–Wallis	0.00171
Canopy closure index	0.0359	0.774	Kruskal–Wallis	0.413
Humus content (%)	0.00499	0.540	Kruskal–Wallis	0.0241
Soil pH	0.111	0.717	ANOVA	0.993
NDVI	0.0319	0.0206	Kruskal–Wallis	0.348
NDMI	0.0752	0.204	ANOVA	0.213
NBR	0.155	0.0245	Kruskal–Wallis	0.239

The analysis revealed that for most variables—including the densities of healthy and damaged saplings, the proportion of surviving trees, and the soil humus content—the assumptions of normality and/or homogeneity of variance were violated. This justified the predominant use of nonparametric tests when comparing burn severity classes.

Significant differences among burn severity classes were identified for several variables, including the densities of healthy and damaged saplings and the proportion of surviving trees (Kruskal–Wallis test, $p < 0.05$). In contrast, no statistically significant differences were observed for canopy closure, NDVI, NDMI, or NBR. Detailed test statistics (H/F values and degrees of freedom) are provided in Table 6.

The direct results of groupwise comparisons of field-based, soil, and satellite-derived indicators are presented in Table 7.

Table 7. Comparison of field and remote-sensing indicators across fire groups (means ± SDs; n in brackets).

Indicator	Background (n = 13)	Low–Moderate (n = 6)	High (n = 3)	Test
Healthy saplings (thous/ha)	6.88 ± 8.87	51.22 ± 56.57	38.33 ± 16.07	Kruskal–Wallis
Damaged saplings (thous/ha)	0.00 ± 0.00	6.17 ± 7.19	33.67 ± 48.99	Kruskal–Wallis
Surviving trees (%)	0.00 ± 0.00	29.17 ± 43.41	56.00 ± 22.54	Kruskal–Wallis
Canopy closure index	0.61 ± 0.10	0.67 ± 0.10	0.57 ± 0.15	Kruskal–Wallis
Humus (%)	2.19 ± 0.63	2.57 ± 0.96	4.77 ± 1.12	Kruskal–Wallis
Soil pH	6.61 ± 0.40	6.58 ± 0.45	6.60 ± 0.36	ANOVA
NDVI	0.71 ± 0.08	0.57 ± 0.24	0.76 ± 0.19	Kruskal–Wallis
NDMI	−0.10 ± 0.18	−0.16 ± 0.32	0.17 ± 0.44	ANOVA
NBR	0.41 ± 0.14	0.20 ± 0.33	0.49 ± 0.32	Kruskal–Wallis

Note: Healthy and damaged saplings were calculated as the sum across height classes and regeneration origin categories reported in Table 1.

The statistically significant differences among the burn severity classes identified in Table 3 are clearly manifested in the forest stand structure and natural regeneration characteristics of the individual sampling plots. Stand density and regeneration metrics display substantial interplot variability, which is driven primarily by fire type and the time elapsed since pyrogenic disturbance.

The sampling plots assigned to the high-burn severity class presented the lowest regeneration potential. In particular, in plot 5, natural regeneration was either absent or represented by extremely sparse sapling densities. A comparable pattern was observed in plot 2 (surface fire of moderate to high intensity, 2022), where both healthy and damaged sapling densities remained low, indicating an early postfire recovery stage with limited establishment success.

In contrast, plots affected by older fire events presented markedly higher regeneration indicators. In plot 4 (moderate-intensity crown fire, 2004), the presence of viable saplings of Scots pine (*Pinus sylvestris* L.) and aspen (*Populus tremula* L.) was documented. Fourteen to fifteen years after fire, the Scots pine (*Pinus sylvestris* L.) sapling density in plot 21 (fire in 2009) reached approximately 40 thousand stems ha^{-1}, whereas plots 19 and 20 supported densities of approximately 20 thousand stems ha^{-1}. These differences highlight divergent postfire recovery trajectories under comparable regional conditions. These differences confirm that forest stand recovery should be considered a dynamic process in which burn severity determines the initial state of the system, while time since fire defines the degree of recovery.

Across all the sampling plots, regeneration was dominated by Scots pine (*Pinus sylvestris* L.), birch (*Betula* spp.), and aspen (*Populus tremula* L.). In the birch-dominated

stands, regeneration occurred predominantly through vegetative (coppice) reproduction rather than through seed-based recruitment, a pattern clearly illustrated in Figure 7.



Figure 7. Origin of the Birch saplings. Scale bar = 10 cm. Source: Original field photograph taken by the authors during the 2023–2025 field campaigns in the Kostanay Region. The image is original and published under the Creative Commons Attribution (CC BY 4.0) licence.

The distribution of healthy and damaged saplings across the sampling plots was characterized by pronounced spatial heterogeneity, with localized density maxima and areas exhibiting little to no regeneration (Figure 8).

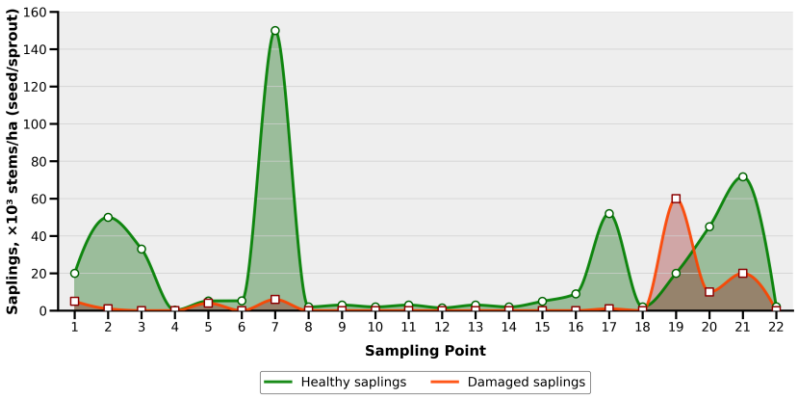


Figure 8. Distribution of healthy and damaged pine saplings across postfire sampling points.

These patterns indicate that vegetation recovery is spatially heterogeneous and strongly controlled by burn severity, with higher NDVI values corresponding to areas characterized by more favourable postfire regeneration conditions.

In addition, the canopy closure index varied among the sampling plots (Table 1). The data presented in Figure 7 indicate that differences in sapling density and condition occur across a wide range of canopy closure values, suggesting that regeneration patterns are not linearly constrained by overstory closure alone.

The pronounced spatial heterogeneity observed in regeneration parameters and stand structure necessitated their formalized comparison across burn severity classes. The most distinct differences were detected between the high-burn-severity sites and the reference or low–moderate-severity groups.

The density of viable saplings differed significantly among the burn severity classes (Kruskal–Wallis test, $p < 0.05$). The density of viable saplings differed significantly among the burn severity classes (Kruskal–Wallis test, $p < 0.05$). The mean values were highest at

sites affected by low–moderate severity fires (mean = XX, 95% CI: XX–XX), whereas high severity burn areas presented greater variability and, in several cases, reduced densities of healthy saplings. Moreover, the proportion of damaged saplings increased with increasing burn severity, reaching maximum values within the high-severity fire class ($p < 0.001$).

The proportion of surviving trees also differed significantly among the groups ($p < 0.01$), reflecting differences in stand retention under varying levels of fire impact. In contrast, the canopy closure index did not significantly differ among the burn severity classes ($p > 0.05$), indicating the limited sensitivity of this metric to the burn severity gradient within the study area.

Comparisons of the spectral indices NDVI, NDMI, and NBR did not reveal statistically significant differences among the burn severity groups ($p > 0.05$), despite differences in median values and ranges. This pattern reflects substantial within-group variability in satellite-derived indicators.

Contrasting patterns of postfire recovery at the local scale are illustrated by a comparison of sampling plots 1 and 2, both of which were affected by fire events in 2023 (Table 8).

Table 8. Comparative characteristics of Sampling Points 1 and 2 (postfire regeneration, 2023).

Sampling Point	Fire Type (2023)	Fire Intensity	Healthy Saplings (thous/ha)	Damaged Saplings (thous/ha)	Regeneration Characteristics
1	Crown fire	Moderate	20	5	Slow recovery; low density of healthy saplings and high proportion of damaged individuals indicate suppressed regeneration.
2	Surface fire	Low	50	1	Rapid recovery; low damage level and high sapling density promote favourable regeneration dynamics.

Despite comparable time intervals since disturbance, the site affected by a low-intensity surface fire presented a greater density of viable saplings and a lower proportion of damaged individuals than did the plot subjected to a moderate-intensity crown fire did. This example demonstrates that differences in postfire regeneration parameters persist at the level of individual sampling plots and reflect pronounced spatial heterogeneity in recovery processes. Similar variability was observed across the other sites, where contrasting combinations of sapling density, proportions of damaged individuals, and degrees of stand retention were recorded.

Overall, the results of the groupwise comparisons (Table 3) confirmed that the natural regeneration parameters were the most sensitive indicators along the burn severity gradient, whereas the canopy closure index did not significantly differ among the fire intensity classes.

The observed interplot variability in regeneration characteristics further indicates that differences in sapling structure and condition cannot be explained solely by burn severity gradients. Accordingly, subsequent analyses focused on the soil conditions at the sampling plots and their relationships with postfire regeneration metrics. The associations between edaphic characteristics and the density of viable saplings are illustrated in Figure 9.

The observed distribution of NDMI values highlights the critical role of moisture availability in postfire recovery, indicating that sites with higher moisture levels support more stable and efficient vegetation regeneration processes.

The relationships between the soil characteristics and natural regeneration parameters are illustrated in Figure 9. The data show that the viable sapling density varies across a wide

range of soil humus contents. In general, higher densities of healthy saplings are associated with increased humus content, whereas soils with low organic matter content are characterized by sparse and spatially heterogeneous regeneration patterns. Notably, at several sampling plots, the sapling density remained low or close to zero despite comparable time intervals since the fire, highlighting pronounced interplot variability in recovery outcomes.

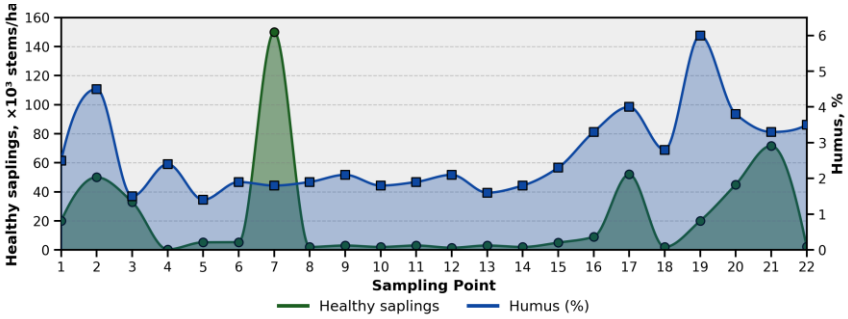


Figure 9. Relationships between the viable sapling density and soil humus content in postfire sampling plots.

In plots where the soil humus content exceeded approximately 2.5–3.0%, some of the highest viable sapling densities were recorded, whereas sites with minimal humus content exhibited regeneration limited to isolated individuals or the complete absence of saplings. Similar differences were observed among plots belonging to the same burn severity class, indicating that local soil conditions substantially contributed to the observed variability in postfire regeneration beyond the effect of fire alone.

Overall, the analysis of field-based and soil indicators demonstrated that differences in the structure and conditions of postfire regeneration are shaped by the combined effects of fire impact and local site conditions. To assess the extent to which these patterns are reflected in remote sensing data and can be detected at broader spatial scales, the satellite-derived indices NDVI, NDMI, and NBR were subsequently examined. The distributions of the spectral index values across the burn severity classes are presented in Figure 10.

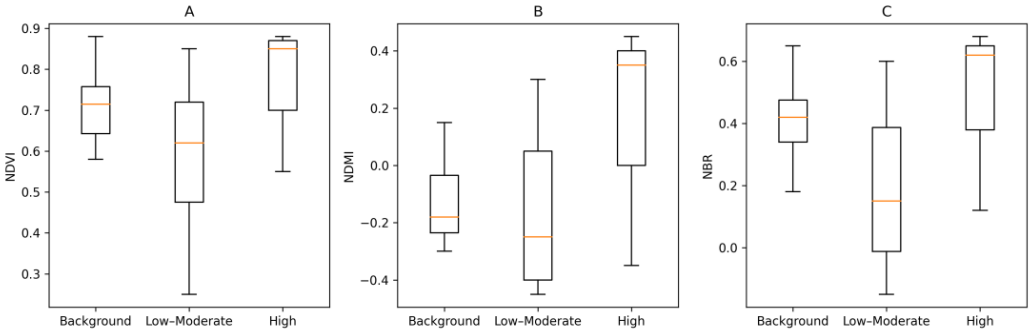


Figure 10. Distributions of spectral indices across fire severity groups: (**A**) NDVI; (**B**) NDMI; and (**C**) NBR. The boxplots illustrate the median, interquartile range, and outliers for each fire severity class (Background, Low–Moderate, and High). These results suggest that regeneration success is closely linked to burn severity, with low–moderate severity fires promoting more favourable conditions for the establishment and growth of saplings.

As shown in the figure, the distributions of the NDVI, NDMI, and NBR are characterized by pronounced within-group variability. Reference sites and areas affected by low–moderate-intensity fires generally present higher median NDVI and NBR values than high-intensity burn areas do, whereas the NDMI displays a wide range of variation, reflecting heterogeneity in postfire moisture conditions across the landscape.

The observed patterns of regeneration correspond well with findings reported in recent studies, indicating higher recovery rates after low- and moderate-intensity fires and reduced regeneration following high-severity disturbances [1,76,77].

Despite differences in median values and variability ranges, no statistically significant differences in spectral indices were detected among burn severity classes (Table 2), indicating substantial spatial heterogeneity of satellite-derived indicators within groups. At the level of individual sampling plots, however, contrasting index values were observed even within similar burn severity classes. For example, plots 19 and 20, affected by surface fires, presented some of the highest spectral index values, whereas plots 5 and 7, subjected to crown fires, presented reduced NBR and NDMI values, reflecting more severe vegetation disturbance. These examples underscore the high interplot variability of satellite-derived metrics and highlight the limitations of their interpretation in the absence of field-based validation.

Accordingly, subsequent analyses focused on the relationships among field-based recovery indicators, soil properties, and satellite-derived spectral indices. Correlation analysis was performed using Spearman's rank correlation coefficient (r), which was calculated at the level of the sampling plots (n = 22) because of the nonnormal distribution of some variables and differences in measurement scales.

The identified correlations highlight the interconnected nature of soil properties and vegetation recovery, indicating that both edaphic conditions and fire effects jointly determine regeneration outcomes.

Only quantitative ecological variables were included in the correlation analysis: the density of viable saplings (ind./ha), the proportion of surviving trees (%), the occurrence frequency of regeneration (%), the humus content (%), and soil acidity (pH), as well as the satellite-derived indices NDVI, NDMI, and NBR. The variable "plot" was used exclusively as an identifier of the sampling plots and was not included in the correlation matrix, as it does not represent a quantitative ecological parameter. Control (unburned) plots were included in the analysis as part of the overall gradient of recovery conditions.

The results are presented in the correlation matrix (Figure 11), which reflects the structure of the relationships among the field-based recovery indicators, soil properties, and spectral indices.

The strongest positive correlations were observed among the spectral indices, particularly between the NDVI and NBR (r = 0.98) and between the NDMI and NDVI (r = 0.63) and between the NDMI and NBR (r = 0.62), indicating consistent changes in vegetation conditions and moisture availability.

The density of viable saplings showed a moderate positive relationship with the satellite-derived indices (NDVI, NBR, and NDMI), as well as with the soil humus content (r = 0.54), suggesting a combined influence of vegetation conditions and soil fertility on postfire recovery success. The proportion of surviving trees also exhibited positive correlations with the spectral indices, particularly the NDVI and NBR, reflecting the relationship between stand retention and remotely sensed vegetation characteristics.

Edaphic variables demonstrated consistent but generally weaker relationships with the spectral indices. The humus content was positively correlated with the NDMI (r = 0.68) and the NDVI (r = 0.48), whereas the soil pH was weakly to moderately correlated with the NDMI (r = 0.50) and the NDVI (r = 0.17). In contrast, the occurrence frequency of regeneration did not significantly correlate with either field-based or satellite-derived indicators.

Overall, the correlation analysis confirms the consistency between ground-based indicators of postfire recovery and integrated satellite-derived measures of vegetation conditions while highlighting the multifactorial nature of the spatial variability of recovery processes.

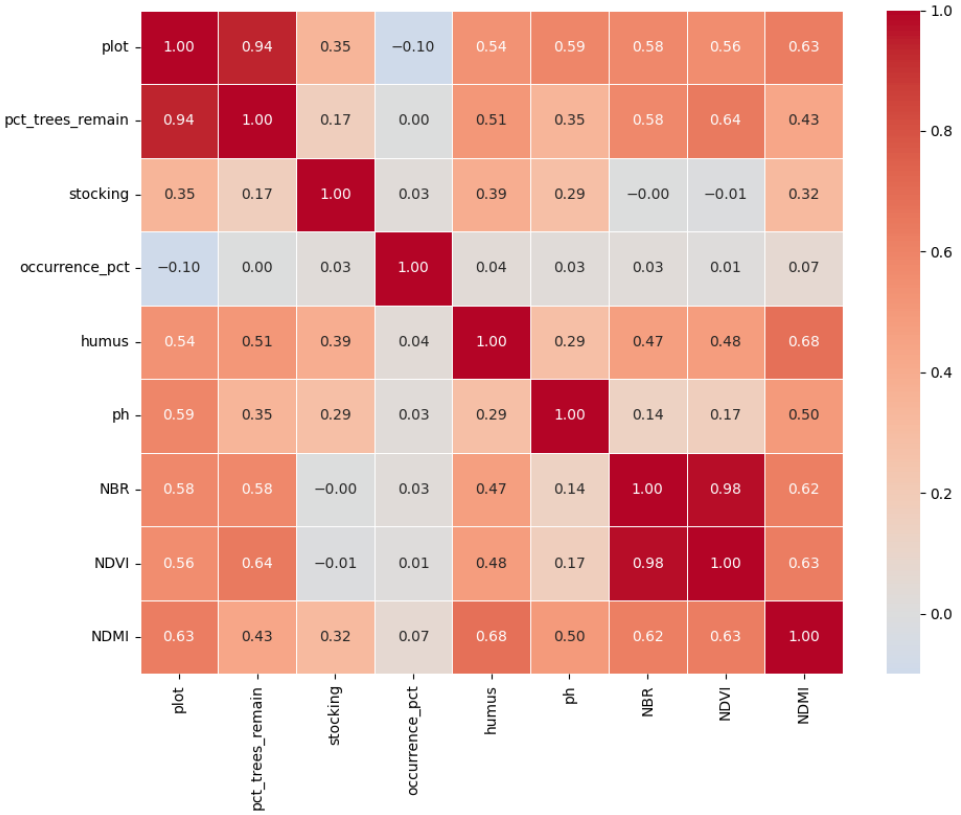


Figure 11. Correlation matrix of field-based and remote-sensing indicators of postfire recovery (Spearman's r).

To further clarify the nature of these relationships and their manifestation at the level of individual variables, direct associations between key field-based and satellite-derived indicators were examined, as shown in Figure 12.

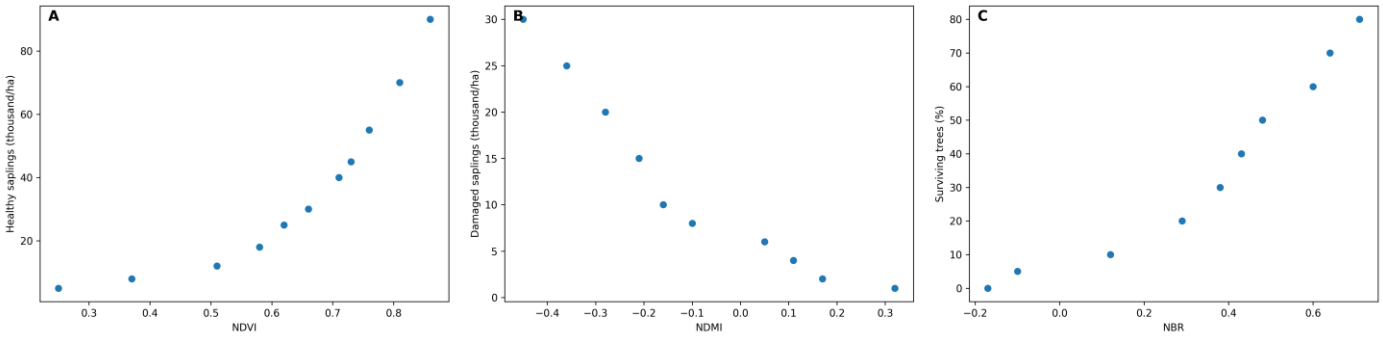


Figure 12. Relationships between field-based and satellite-derived indicators of postfire recovery. (**A**) NDVI vs. healthy sapling density; (**B**) NDMI vs. damaged saplings; (**C**) NBR vs. surviving trees.

The relationships shown in Figure 12 represent bivariate associations between variables based on Spearman correlation analysis. No predictive or regression models were fitted; the plots are provided solely for visualization of monotonic relationships between field-based and satellite-derived indicators.

As shown in Figure 12, the relationships between field-based and satellite-derived indicators demonstrate a high degree of consistency between ground observations and remote sensing data. NDVI values increase with increasing density of viable saplings, and NDMI values decrease with increasing proportion of damaged saplings, whereas NBR is positively correlated with the proportion of surviving trees. These relationships indicate

that integrated satellite indices capture the spatial variability in vegetation conditions and regeneration structure observed during field surveys.

Taken together, the results indicate that postfire forest ecosystem recovery is characterized by pronounced spatial heterogeneity, which is consistently reflected in both ground-based indicators of vegetation structure and condition and in satellite-derived indices.

4. Discussion

The Results section presents empirical patterns derived from field-based, soil, and satellite data without addressing underlying causal mechanisms. Below, these relationships are interpreted within the framework of contemporary fire ecology and postfire successional theory.

The findings indicate that postfire recovery of Scots pine forests in the Kostanay Region of northern Kazakhstan over the examined time frame is governed by the combined effects of burn severity, local soil–hydrological conditions, retention of seed-bearing trees, and regional climatic constraints [78]. This multicomponent control of regeneration is consistent with the concepts of ecosystem resilience and ecological memory, in which fire is viewed not as a single disturbance event but as a process that shapes the long-term developmental trajectories of forest communities [9,13,79].

In comparison with recent studies employing similar combinations of field surveys and remote sensing approaches, the patterns identified in this study are highly consistent and reveal region-specific characteristics. For example, studies based on Landsat-derived indices have demonstrated that postfire recovery trajectories are strongly controlled by burn severity and moisture availability [80–82]. Our results confirm these findings, particularly in terms of the strong agreement between the NDVI/NBR and field-based indicators of vegetation recovery.

Moreover, the magnitude of regeneration decline observed under high-intensity fires in this study is more pronounced than that reported in more humid boreal regions, which may be explained by the lower water-holding capacity of sandy soils and stronger moisture limitation in northern Kazakhstan. This highlights the importance of the regional environmental context in modulating postfire recovery processes.

In addition to the general agreement with previous studies, our results provide further quantitative support for the relationship between burn severity and regeneration success under comparable methodological frameworks. Similar patterns have been reported in the boreal forests of Canada and Siberia, where high-severity fires have been shown to substantially reduce conifer regeneration due to the loss of seed sources and increased moisture limitation. Under such conditions, shifts in successional trajectories are observed, including transitions toward deciduous-dominated stands or even nonforest vegetation, reflecting the development of alternative stable ecosystem states [83–85].

The contemporary literature further emphasizes that regeneration success is determined not only by overall fire intensity but also by the spatial heterogeneity of postfire microsites, including canopy gaps, localized patches of mineral soil exposure, and remnants of intact litter layers [86,87].

While the observed positive response of Scots pine regeneration to low- and moderate-intensity fires is consistent with the findings of previous studies, some studies have reported successful regeneration even after high-severity fires under favourable climatic conditions and sufficient seed availability. In contrast, our results indicate that under the arid conditions of the study region, high-intensity fires more frequently lead to suppressed regeneration and potential shifts toward alternative vegetation states. This discrepancy suggests that climatic constraints and soil moisture availability play a more decisive role in semiarid boreal systems than in more humid regions.

These patterns indicate that the response of postfire recovery is not linear but depends on threshold effects associated with burn severity. In particular, the transition from moderate to high burn severity represents a critical point beyond which regeneration processes become strongly constrained, leading to increased variability and divergence in successional trajectories.

Thus, high burn severity corresponds to a greater "disturbance dose," leading to the development of alternative recovery trajectories, whereas low burn severity creates conditions for a more rapid return to the predisturbance state of the ecosystem.

The importance of soil factors revealed by statistical analysis aligns with global studies of postfire ecosystem dynamics. The positive relationships between the humus content, soil pH, and sapling density highlight the role of organic matter and soil reactions in enhancing the soil WHC and seedling survival [78]. This is consistent with the results presented in the Results section, which showed that sites with higher NDVI and NDMI values are characterized by greater densities of viable saplings and more favourable recovery conditions. Conversely, the negative association between sapling density and the dominance of sandy fractions underscores the limiting role of low substrate water retention, which is characteristic of dry boreal and subboreal ecosystems [88,89].

The integration of field observations with remote sensing data allowed for a more nuanced interpretation of postfire recovery patterns. The positive relationship between the NDVI and the density of viable saplings reflects increasing productive biomass as young tree cohorts become established and expand [57]. In contrast, the negative association between the NDMI and the proportion of damaged saplings highlights the critical role of water stress in constraining plant survival during the early stages of postfire recovery [58]. The positive relationship between the NBR and the proportion of surviving trees further confirms the applicability of this index for assessing stand retention and residual forest structure following fire disturbance [36].

Importantly, the temporal dynamics of the NDVI and NBR primarily capture changes in canopy reflectance and structural development, whereas the Scots pine sapling density derived from field surveys represents later successional stages and may respond with a temporal lag relative to satellite-detected recovery signals. This temporal decoupling should be considered when discrepancies between ground-based regeneration metrics and remotely sensed indices are interpreted.

Overall, the identified relationships demonstrate a high degree of consistency between field-based and satellite-derived indicators, supporting the validity of integrated approaches for monitoring postfire ecosystem recovery [22,23].

The strong agreement between field observations and satellite-derived indices supports the reliability of remote sensing techniques for monitoring postfire dynamics [20,87]. Similar conclusions have been reported in studies emphasizing the importance of integrating ground-based and remote sensing data [77].

In addition to abiotic drivers, biotic constraints may play a significant role in shaping postfire recovery trajectories. During field surveys, the presence of the fungus Rhizina undulata was documented at several sites (Figure 13), a species typically associated with strongly heated and severely burned soils. Its occurrence suggests the presence of additional biological stressors that may suppress seedling establishment and further delay forest regeneration under conditions of high fire severity.



Figure 13. Sampling point 1, Rhizina undulata fungus. Scale bar = 5 cm. Source: Original field photograph taken by the authors during the 2025 field campaign in the Kostanay Region. The image is original and published under the Creative Commons Attribution (CC BY 4.0) licence.

This species is recognized as a pyrogenic pathogen of coniferous trees and is capable of infecting root systems, thereby reducing sapling viability even under relatively favourable edaphic conditions [90,91]. The occurrence of R. undulata underscores the need to account for biotic stressors alongside abiotic drivers when evaluating the regenerative potential of burned forest sites.

The integrated analysis of field-based, soil, and remote sensing indicators reveals the emergence of a coherent gradient of postfire recovery. Within this gradient, the combination of moderate burn severity, elevated soil humus content, and favourable values of satellite-derived indices corresponds to the most successful regeneration trajectories. At the opposite end of the spectrum are sites characterized by high burn severity, pronounced moisture limitation, and minimal densities of viable saplings. These patterns are consistent with the concept of alternative stable states in boreal forest ecosystems, whereby severe disturbances can redirect successional pathways away from prefire forest conditions [13,92].

These findings are consistent with recent studies that have demonstrated strong correlations between the NDVI, NDMI, and field-based regeneration metrics in postfire landscapes [93]. Moreover, our results highlight that in heterogeneous and moisture-limited environments, satellite-derived indices may exhibit substantial within-group variability, which can obscure statistically significant differences among fire intensity classes despite clear ecological trends observed in field data.

Within the proposed dose–response framework, these findings can be interpreted as evidence that increasing fire intensity leads to nonlinear changes in recovery trajectories, with threshold-like transitions occurring under high-severity conditions. These findings support the view that postfire recovery in arid boreal ecosystems is not only intensity dependent but also strongly constrained by environmental thresholds related to moisture availability and soil properties.

Several limitations of the present study should be acknowledged, including the limited number of high-severity burn sites and the focus on early to midterm stages of postfire recovery. These constraints should be considered when the findings are extrapolated to longer temporal scales or to other regions with differing climatic or geomorphological settings.

Overall, this study advances the understanding of postfire recovery processes in arid boreal ecosystems of northern Kazakhstan and highlights that the regeneration trajectories of Scots pine forests are shaped by interactions among fire regime characteristics, the soil

water balance, biotic constraints, and the persistence of seed sources. These insights have direct practical relevance for the development of adaptive forest management strategies under conditions of increasing fire frequency and intensity.

Accordingly, the obtained results should be interpreted as a spatial approximation of temporal recovery dynamics rather than as a direct representation of continuous successional trajectories.

5. Conclusions

This study, which is based on the integration of field observations, soil data, and remote sensing materials, provides a comprehensive and statistically robust assessment of the factors controlling postfire recovery of Scots pine forests in the Kostanay region. Analysis of 22 sampling plots grouped into three fire intensity classes (reference conditions, low–moderate, and high burn severity) revealed consistent patterns of forest regeneration and their relationships with fire regime characteristics, edaphic conditions, and spectral properties of vegetation cover.

The main conclusions of the study are as follows:

1. Burn severity is a key and statistically significant factor in determining the direction and rate of postfire recovery of Scots pine forests in northern Kazakhstan. Its influence operates through interactions with soil–hydrological conditions, the preservation of seed sources, and regional climatic constraints.
2. The most favourable conditions for the natural regeneration of Scots pine (*Pinus sylvestris* L.) occur after low and moderate burn severity. These sites are characterized by high densities of viable saplings, lower proportions of damaged individuals, and partial preservation of the organic soil horizon and seed-bearing trees, resulting in stable and resilient regeneration trajectories.
3. High burn severity significantly reduces the regenerative potential of forest ecosystems, resulting in delayed and spatially heterogeneous recovery, a high proportion of damaged saplings, and shifts in successional trajectories toward deciduous or sparsely forested communities. These findings resolve previously reported inconsistencies by demonstrating that low and moderate burn severity, rather than high severity conditions, create the most resilient conditions for the recovery of Scots pine stands.
4. The satellite-derived indices NDVI, NDMI, and NBR exhibited statistically significant agreement with the field-based indicators, capturing variations in the viable sapling density, degree of sapling damage, and stand retention. This confirms their applicability as reliable proxy indicators for monitoring postfire recovery in arid boreal environments, provided that they are validated through ground-based observations.
5. Soil characteristics—particularly the humus content and soil reaction (pH)—act as statistically significant modifying factors of recovery processes. Under comparable burn severity conditions, more favourable edaphic conditions are associated with higher rates of viable sapling establishment, which is especially critical under the soil moisture deficit conditions characteristic of the study region.
6. Interpretation of the results should account for several limitations, including the limited number of sampling plots within the high-burn severity class, the focus on early to midterm stages of postfire recovery, and uncertainties associated with the spatial resolution of satellite data and the incomplete consideration of biotic factors.
7. The practical implications of this study include the need for differentiated postfire forest management strategies in arid boreal regions. Priority measures should focus on the preservation of seed-bearing trees, prevention of repeated high-intensity fires, and protection of the soil organic horizon to enhance natural regeneration capacity. From a methodological perspective, the integration of field-based observations with satellite-

lite-derived indices (NDVI, NDMI, NBR, and dNBR) provides a reproducible and scalable framework for monitoring postfire recovery. This approach can be applied to other fire-prone regions with similar environmental conditions, provided that satellite data are calibrated and validated using ground-based measurements. The proposed methodology is particularly relevant for large-scale monitoring and management planning as it allows the identification of priority areas for restoration and supports decision-making under conditions of increasing fire frequency and intensity.

8. The results support the applicability of the dose–response framework for analyzing postfire recovery in forest ecosystems and highlight the importance of accounting for temporal dynamics when interpreting successional processes.

Author Contributions: Conceptualization, Z.O. and Z.M.; methodology, Z.O. and Z.M.; software, A.Z., D.A. and M.U.; validation, Z.O., Z.M. and K.T.; formal analysis, M.U. and K.T.; investigation, Z.O., Z.M. and A.Z.; resources, Z.O., Z.M., A.Z. and D.A.; data curation, Z.O., A.Z. and D.A.; writing—original draft preparation, Z.O., Z.M. and A.Z.; writing—review and editing, Z.O., Z.M. and A.Z.; visualization, A.Z., D.A. and M.U.; supervision, Z.O., Z.M. and A.Z.; project administration, Z.O., Z.M. and A.Z.; funding acquisition, Z.O., Z.M., A.Z., M.U. and D.A. All authors have read and agreed to the published version of the manuscript.

Funding: This study was undertaken as part of grant funding for scientists awarded for scientific and/or scientific and technical projects from 2023 to 2025 by the Ministry of Science and Higher Education of the Republic of Kazakhstan (IRN № AP19678305).

Data Availability Statement: The original contributions of this study are presented within the article. Further inquiries can be directed to the corresponding author.

Acknowledgments: The authors express their gratitude to the Ministry of Science and Higher Education of the Republic of Kazakhstan for funding this research. This study was carried out within the framework of grant funding for scientific and/or scientific and technical projects for 2023–2025 (IRN No. AP19678305).

Conflicts of Interest: The authors declare that they have no conflicts of interest.

Appendix A

Table A1. Fire regime and stand structure.

Sampling Point	Species Composition	Most Recent Fire Year	Fire Type	Surviving Trees (% of Prefire)	Stand Density
1	10P	2022	Crown fire (moderate intensity)	0	0.7
2	10P	2022	Running surface fire (moderate–high intensity)	30	0.7
3	8P2B	n/a	Not recorded	Not recorded	0.5
4	7P	2004	Crown fire (moderate intensity)	5	0.6
5	10P	2022	Crown fire (moderate intensity)	Not recorded	0.5
6	10P	n/a	Not recorded	Not recorded	0.5
7	10P	2022	Crown fire (moderate intensity)	Not recorded	0.7
8	10P	n/a	Not recorded	Not recorded	0.7
9	10P	n/a	Not recorded	Not recorded	0.6
10	10P	n/a	Not recorded	Not recorded	0.7
11	10P	n/a	Not recorded	Not recorded	0.5
12	10P	n/a	Not recorded	Not recorded	0.5

Table A1. *Cont.*

Sampling Point	Species Composition	Most Recent Fire Year	Fire Type	Surviving Trees (% of Prefire)	Stand Density
13	10P	n/a	Not recorded	Not recorded	0.5
14	10P	n/a	Not recorded	Not recorded	0.7
15	10B	n/a	Not recorded	Not recorded	0.6
16	8A2B	n/a	Not recorded	Not recorded	0.6
17	10B	2020	Running surface fire	90	0.8
18	10P	n/a	Not recorded	Not recorded	0.7
19	10B	2010	Running surface fire (moderate–high intensity)	70	0.6
20	10B	2010	Running surface fire (moderate–high intensity)	68	0.4
21	10P	2009	Crown fire (moderate intensity)	80	0.7
22	8A2B	Not recorded	Not recorded	Not recorded	0.8

Note: P—pine (*Pinus sylvestris*); B—birch (*Betula* spp.); A—aspen (*Populus tremula*). Species composition is expressed in tenths (e.g., 8A2B = 80% aspen and 20% birch). Stand density indicates canopy closure (0–1). Fire type and year are indicated where available; otherwise, data are marked as "Not recorded".

Table A2. Regeneration structure and species composition.

Sampling Point	Dominant Species	Healthy Saplings (thous./ha, seed/sprout)	Damaged Saplings (thous./ha, seed/sprout)	Occurrence (%)
1	Pine (*Pinus sylvestris*)	20/0	5/0	100
2	Pine (*Pinus sylvestris*)	50/0	1/0	100
3	Pine (*Pinus sylvestris*)	20/0 + 3/0	n/a	80
	Birch (*Betula* spp.)	10/0	n/a	20
4	Pine (*Pinus sylvestris*)	0.2/0	n/a	70
	Aspen (*Populus tremula*)	0.1/0	n/a	1
5	Pine (*Pinus sylvestris*)	5/0	4/0	90
	Birch (*Betula* spp.)	0/2	0/1	10
6	Pine (*Pinus sylvestris*)	5/0	n/a	90
	Birch (*Betula* spp.)	0/3	n/a	10
7	Pine (*Pinus sylvestris*)	150/0	6/0	100
8	Pine (*Pinus sylvestris*)	2/0	n/a	100
9	Pine (*Pinus sylvestris*)	3/0	n/a	100
10	Pine (*Pinus sylvestris*)	1/0 + 1/0	n/a	100
11	Pine (*Pinus sylvestris*)	2/0 + 1/0	n/a	100
12	Pine (*Pinus sylvestris*)	0.5/0 + 1/0	n/a	100
13	Pine (*Pinus sylvestris*)	2/0 + 1/0	n/a	100
14	Pine (*Pinus sylvestris*)	1/0 + 1/0	n/a	100
15	Birch (*Betula* spp.)	0/2 + 0/3	n/a	100
16	Aspen (*Populus tremula*)	7/0	n/a	80
	Birch (*Betula* spp.)	0/2	n/a	20
17	Birch (*Betula* spp.)	0/50 + 0/2	1/0	100
18	Pine (*Pinus sylvestris*)	1/0 + 1/0	n/a	100
19	Birch (*Betula* spp.)	0/20	0/30 + 60/0	100
20	Birch (*Betula* spp.)	0/20 + 0/25	10/0	100
21	Pine (*Pinus sylvestris*)	40/0	20/0	80
	Aspen (*Populus tremula*)	30/0	n/a	10
	Birch (*Betula* spp.)	1/0 + 0/7	n/a	10
22	Aspen (*Populus tremula*)	2/0 + 0/8	n/a	60
	Birch (*Betula* spp.)	0/6	n/a	40

Note: Seed-origin and sprout-origin refer to the biological origin of saplings. Occurrence (%) represents the spatial distribution frequency of saplings within the sampling plot. Values are expressed as seed-origin/sprout-origin saplings. Multiple values indicate different cohorts or microsites within the sampling plot.

Table A3. Edaphic properties and spectral indices.

Sampling Point	Humus (%)	Soil pH	NBR	NDVI	NDMI
1	2.5	7.2	0.003	0.51	−0.36
2	4.5	6.3	0.12	0.54	−0.34
3	1.5	6.1	0.18	0.58	−0.22
4	2.4	6.1	0.43	0.72	−0.12
5	1.4	6.7	−0.10	0.37	−0.45
6	1.9	5.9	0.47	0.75	−0.23
7	1.8	6.2	−0.17	0.25	−0.44
8	1.9	6.3	0.29	0.62	−0.21
9	2.1	6.4	0.20	0.66	−0.23
10	1.8	6.5	0.48	0.71	−0.10
11	1.9	6.8	0.38	0.68	−0.16
12	2.1	6.8	0.45	0.76	−0.16
13	1.6	6.2	0.43	0.72	−0.28
14	1.8	7.0	0.43	0.72	−0.19
15	2.3	7.1	0.40	0.75	−0.09
16	3.3	7.0	0.66	0.88	0.06
17	4.0	6.3	0.62	0.86	0.32
18	2.8	6.8	0.60	0.81	0.33
19	6.0	6.5	0.64	0.86	0.35
20	3.8	7.0	0.71	0.87	0.49
21	3.3	7.0	0.40	0.73	0.11
22	3.5	7.0	0.34	0.65	0.13

Note: All values represent mean measurements obtained from approximately 80 sampling points within each plot. Remote sensing indices (NDVI, NDMI, NBR) were derived from Landsat 8 OLI imagery.

References

1. Mantero, G.; Morresi, D.; Negri, S.; Anselmetto, N.; Lingua, E.; Bonifacio, E.; Garbarino, M.; Marzano, R. Short-term drivers of postfire forest regeneration in the Western Alps. *Fire Ecol.* **2023**, *19*, 23. [CrossRef]
2. Diaz, L.R.; Delcourt, C.J.F.; Langer, M.; Loranty, M.M.; Rogers, B.M.; Scholten, R.C.; Shestakova, T.A.; Talucci, A.C.; Vonk, J.E.; Wangchuk, S.; et al. Environmental drivers and remote sensing proxies of postfire thaw depth in eastern Siberian larch forests. *Earth Syst. Dyn.* **2024**, *15*, 1459–1478. [CrossRef]
3. Pérez-Cabello, F.; Serrano-Notivoli, R.; Montorio, R.; Iranzo, C. The climate-fire nexus: Understanding postfire vegetation recovery. *For. Ecol. Manag.* **2026**, *606*, 123568. [CrossRef]
4. IPCC. Climate Change 2021: The Physical Science Basis. In *Contribution of Working Group I to the Sixth Assessment Report of the Intergovernmental Panel on Climate Change*; Cambridge University Press: Cambridge, UK, 2021.
5. Jolly, W.M.; Cochrane, M.A.; Freeborn, P.H.; Holden, Z.A.; Brown, T.J.; Williamson, G.J.; Bowman, D.M.J.S. Climate-induced variations in global wildfire danger from 1979 to 2013. *Nat. Commun.* **2015**, *6*, 7537. [CrossRef]
6. Westerling, A.L. Increasing western US forest wildfire activity: Sensitivity to changes in the timing of spring. *Philos. Trans. R. Soc. B Biol. Sci.* **2016**, *371*, 20150178.
7. Abatzoglou, J.T.; Williams, A.P. Impact of anthropogenic climate change on wildfire across western US forests. *Proc. Natl. Acad. Sci. USA* **2016**, *113*, 11770–11775. [CrossRef]
8. Turner, M.G.; Braziunas, K.H.; Hansen, W.D.; Harvey, B.J. Short-interval severe fire erodes the resilience of subalpine lodgepole pine forests. *Proc. Natl. Acad. Sci. USA* **2019**, *116*, 11319–11328. [CrossRef] [PubMed]
9. Bowman, D.M.J.S.; Balch, J.K.; Artaxo, P.; Bond, W.J.; Carlson, J.M.; Cochrane, M.A.; D'Antonio, C.M.; DeFries, R.S.; Doyle, J.C.; Harrison, S.P.; et al. Fire in the Earth system. *Science* **2009**, *324*, 481–484. [CrossRef] [PubMed]
10. Keeley, J.E.; Bond, W.J.; Bradstock, R.A.; Pausas, J.G.; Rundel, P.W. *Fire in Mediterranean Ecosystems: Ecology, Evolution and Management*; Cambridge University Press: Cambridge, UK, 2012.
11. Stevens, J.T.; Safford, H.D.; Harrison, S.; Latimer, A.M. Forest disturbance accelerates thermophilization of understory plant communities. *J. Ecol.* **2017**, *105*, 434–445.
12. Coop, J.D.; Parks, S.A.; Stevens-Rumann, C.S.; Crausbay, S.D.; Higuera, P.E.; Hurteau, M.D.; Tepley, A.; Whitman, E.; Assal, T.; Collins, B.M.; et al. Wildfire-driven forest conversion in western North American landscapes. *BioScience* **2020**, *70*, 659–673. [CrossRef]
13. Agee, J.K. *Fire Ecology of Pacific Northwest Forests*; Island Press: Washington, DC, USA, 1993.

14. Turner, M.G.; Baker, W.L.; Peterson, C.J.; Peet, R.K. Factors influencing succession: Lessons from large, infrequent natural disturbances. *Ecosystems* **1998**, *1*, 511–523. [CrossRef]
15. Harvey, B.J.; Donato, D.C.; Turner, M.G. High-severity fire creates a distinct early successional pathway in a mixed-conifer forest. *Ecol. Appl.* **2016**, *26*, 1846–1860. [CrossRef]
16. Johnstone, J.F.; Allen, C.D.; Franklin, J.F.; Frelich, L.E.; Harvey, B.J.; Higuera, P.E.; Mack, M.C.; Meentemeyer, R.K.; Metz, M.R.; Perry, G.L.W.; et al. Changing disturbance regimes, ecological memory, and forest resilience. *Front. Ecol. Environ.* **2016**, *14*, 369–378. [CrossRef]
17. Miller, J.D.; Thode, A.E. Quantifying burn severity in a heterogeneous landscape with a relative version of the delta Normalized Burn Ratio (dNBR). *Remote Sens. Environ.* **2007**, *109*, 66–80. [CrossRef]
18. Parks, S.A.; Miller, C.; Parisien, M.A.; Holsinger, L.M.; Dobrowski, S.Z.; Abatzoglou, J.T. Wildland fire deficit and surplus in the western United States, 1984–2012. *Ecosphere* **2015**, *6*, 275. [CrossRef]
19. Bissenbayeva, S.; Melisbek, S.; Baymukan, E. An overview of forest monitoring in Kazakhstan based on Earth observation. *Bulletin of the L.N. Gumilyov Eurasian National University. Chem. Geogr. Ecol. Ser.* **2024**, *147*, 135–149.
20. Xu, E.; Wulder, M.A.; White, J.C.; Hermosilla, T.; Coops, N.C.; Hobart, G.W.; Bolton, D.K. Assessing burn severity and vegetation restoration in Alberta's boreal forests following the 2016 Fort McMurray wildfire: A remote sensing time-series study. *Can. J. Remote Sens.* **2024**, *10*, 2361569. [CrossRef]
21. Cohen, W.B.; Yang, Z.; Stehman, S.V.; Schroeder, T.A.; Bell, D.M.; Masek, J.G.; Huang, C.; Meigs, G.W. Forest disturbance across the conterminous United States from 1985–2012: The emerging dominance of forest decline. *For. Ecol. Manag.* **2016**, *360*, 242–252. [CrossRef]
22. Gitas, I.Z.; Mitri, G.H.; Veraverbeke, S.; Polychronaki, A. Advances in remote sensing of postfire vegetation recovery monitoring: A review. In *Remote Sensing of Biomass: Principles and Applications*; Fatoyinbo, L., Ed.; InTech: Rijeka, Croatia, 2012; pp. 143–176.
23. Chu, T.; Guo, X. Remote sensing techniques in monitoring postfire effects and patterns of forest recovery in boreal forest regions: A review. *Remote Sens.* **2014**, *6*, 470–520. [CrossRef]
24. Banskota, A.; Kayastha, N.; Falkowski, M.J.; Wulder, M.A.; Froese, R.E.; White, J.C. Forest monitoring using Landsat time series data: A review. *Can. J. Remote Sens.* **2014**, *40*, 362–384. [CrossRef]
25. Zhu, Z. Change detection using Landsat time series: A review of frequencies, preprocessing, algorithms, and applications. *ISPRS J. Photogramm. Remote Sens.* **2017**, *130*, 370–384.
26. Tewkesbury, A.P.; Comber, A.J.; Tate, N.J.; Lamb, A.; Fisher, P.F. A critical synthesis of remotely sensed optical image change detection techniques. *Remote Sens. Environ.* **2015**, *160*, 1–14.
27. Hirschmugl, M.; Gallaun, H.; Dees, M.; Datta, P.; Deutscher, J.; Koutsias, N.; Schardt, M. Methods for mapping forest disturbance and degradation from optical Earth observation data: A review. *Curr. For. Rep.* **2017**, *3*, 32–45. [CrossRef]
28. Bartels, S.F.; Chen, H.Y.H.; Wulder, M.A.; White, J.C. Trends in postdisturbance recovery rates of Canada's forests following wildfire and harvest. *For. Ecol. Manag.* **2016**, *361*, 194–207. [CrossRef]
29. Cohen, W.B.; Healey, S.P.; Yang, Z.; Stehman, S.V.; Brewer, C.K.; Brooks, E.B.; Gorelick, N.; Huang, C.; Hughes, M.J.; Kennedy, R.E.; et al. How similar are forest disturbance maps derived from different Landsat time-series algorithms? *For. Ecol. Manag.* **2017**, *376*, 259–268.
30. Hessl, A.E.; McKenzie, D.; Schellhaas, R. Drought, fire, and forest dynamics in western North America. *Ecol. Appl.* **2012**, *22*, 760–774. [CrossRef]
31. Rogers, B.M.; Soja, A.J.; Goulden, M.L.; Randerson, J.T. Influence of tree species on continental differences in boreal fires and climate feedbacks. *Nat. Geosci.* **2015**, *8*, 228–234. [CrossRef]
32. Food and Agriculture Organization of the United Nations (FAO). *Global Forest Resources Assessment 2023: Country Report—Kazakhstan*; FAO: Rome, Italy, 2023.
33. Pickett, S.T.A.; White, P.S. (Eds.) *The Ecology of Natural Disturbance and Patch Dynamics*; Academic Press: Orlando, FL, USA, 1985.
34. Franklin, J.F.; Spies, T.A.; Van Pelt, R.; Carey, A.B.; Thornburgh, D.A.; Rae Berg, D.; Lindenmayer, D.B.; Harmon, M.E.; Keeton, W.S.; Shaw, D.C.; et al. Disturbances and structural development of natural forest ecosystems with silvicultural implications, using Douglas-fir forests as an example. *For. Ecol. Manag.* **2002**, *155*, 399–423. [CrossRef]
35. *OST 56-69-83*; Sample Forest Inventory Plots: Method of Establishment. Central Bureau of Scientific and Technical Information of Forestry (CBNTIleskhoz): Moscow, Russia, 1984; 11p. (In Russian)
36. Key, C.H.; Benson, N.C. Landscape assessment: Ground measure of severity, the Composite Burn Index, and remote sensing of severity, the Normalized Burn Ratio. In *FIREMON: Fire Effects Monitoring and Inventory System*; Lutes, D.C., Ed.; USDA Forest Service: Fort Collins, CO, USA, 2006; pp. LA1–LA51.
37. Parks, S.A.; Dillon, G.K.; Miller, C. A New Metric for Quantifying Burn Severity: The Relativized Burn Ratio. *Remote Sens.* **2014**, *6*, 1827–1844. [CrossRef]
38. Krebs, C.J. *Ecological Methodology*, 2nd ed.; Benjamin/Cummings: Menlo Park, CA, USA, 1999.

39. Sukachev, V.N.; Zonn, S.V. *Methodological Guidelines for the Study of Forest Types*; Academy of Sciences of the USSR: Moscow, Russia, 1961; 144p. (In Russian)
40. Melekhov, I.S. *Forest Pyrology: A Textbook*; Lesnaya Promyshlennost Publishers: Moscow, Russia, 1983; 60p. (In Russian)
41. Ryan, K.C.; Noste, N.V. Evaluating prescribed fires. In *Proceedings of the Symposium and Workshop on Wilderness Fire*; USDA Forest Service, Intermountain Forest and Range Experiment Station: Missoula, MT, USA, 1985; General Technical Report INT-182; pp. 230–238.
42. Hurlbert, S.H. Pseudoreplication and the design of ecological field experiments. *Ecol. Monogr.* **1984**, *54*, 187–211. [CrossRef]
43. Quinn, G.P.; Keough, M.J. Experimental design and data analysis in ecology and biology. *Trends Ecol. Evol.* **1998**, *13*, 54–55.
44. Underwood, A.J. *Experiments in Ecology: Their Logical Design and Interpretation Using Analysis of Variance*; Cambridge University Press: Cambridge, UK, 1997.
45. Parks, S.A.; Abatzoglou, J.T. Warmer and drier fire seasons contribute to increases in area burned at high severity in western US forests from 1985 to 2017. In *USDA Forest Service General Technical Report*; Rocky Mountain Research Station: Fort Collins, CO, USA, 2020. [CrossRef]
46. Avery, T.E.; Burkhart, H.E. *Forest Measurements*, 5th ed.; Waveland Press: Long Grove, IL, USA, 2015.
47. Certini, G. Effects of fire on properties of forest soils: A review. *Oecologia* **2005**, *143*, 1–10. [CrossRef] [PubMed]
48. Neary, D.G.; Ryan, K.C.; DeBano, L.F. *Wildland Fire in Ecosystems: Effects of Fire on Soil and Water*; General Technical Report RMRS-GTR-42-vol.4; USDA Forest Service, Rocky Mountain Research Station: Ogden, UT, USA, 2005.
49. Roy, D.P.; Boschetti, L.; Trigg, S.N. Remote sensing of fire severity: Assessing the performance of the Normalized Burn Ratio. *Geophys. Res. Lett.* **2006**, *33*, L21401. [CrossRef]
50. Lin, S.; Wang, C.; Li, X.; Zhang, Y.; Liu, H.; Chen, J.; Zhao, F. Characterizing Post-Fire Forest Structure Recovery in the Great Xing'an Mountain Using GEDI and Time Series Landsat Data. *Remote Sens.* **2023**, *15*, 3107. [CrossRef]
51. Pobedinsky, A.V. *Study of Forest Regeneration Processes: Methodological Guidelines*; Siberian Branch of the Academy of Sciences of the USSR: Krasnoyarsk, Russia, 1962; 60p. (In Russian)
52. Republic of Kazakhstan. Forest Code of the Republic of Kazakhstan (No. 477, July 8, 2003). Ministry of Justice of the Republic of Kazakhstan: Astana, Kazakhstan, 2003. Available online: https://adilet.zan.kz/eng/docs/K030000477_ (accessed on 14 April 2026).
53. Roy, D.P.; Kovalskyy, V.; Zhang, H.K.; Vermote, E.F.; Yan, L.; Kumar, S.S.; Egorov, A. Characterization of Landsat-7 to Landsat-8 reflective wavelength and normalized difference vegetation index continuity. *Remote Sens. Environ.* **2016**, *185*, 57–70. [CrossRef]
54. Vermote, E.; Justice, C.; Claverie, M.; Franch, B. Preliminary analysis of the performance of the Landsat 8/OLI land surface reflectance product. *Remote Sens. Environ.* **2016**, *185*, 46–56. [CrossRef]
55. Schroeder, W.; Oliva, P.; Giglio, L.; Quayle, B.; Lorenz, E.; Morelli, F. Active fire detection using Landsat-8/OLI data. *Remote Sens. Environ.* **2016**, *185*, 201–210. [CrossRef]
56. Rouse, J.W.; Haas, R.H.; Schell, J.A.; Deering, D.W. Monitoring vegetation systems in the Great Plains with ERTS. In *Proceedings of the Third Earth Resources Technology Satellite-1 Symposium*; NASA: Washington, DC, USA, 1974; NASA SP-351; pp. 309–317.
57. Pettorelli, N.; Vik, J.O.; Mysterud, A.; Gaillard, J.M.; Tucker, C.J.; Stenseth, N.C. Using the satellite-derived NDVI to assess ecological responses to environmental change. *Trends Ecol. Evol.* **2005**, *20*, 503–510. [CrossRef]
58. Dennison, P.E.; Roberts, D.A.; Peterson, S.H.; Rechel, J. Use of normalized difference water index for monitoring live fuel moisture. *Remote Sens. Environ.* **2005**, *95*, 429–438. [CrossRef]
59. Abdollahi, A.; Vafaeinejad, A.; Akhoondzadeh, M.; Eskandari, M. Challenges and opportunities in remote sensing-based fuel load estimation. *Remote Sens.* **2025**, *17*, 415. [CrossRef]
60. EOS Data Analytics. NDMI: Vegetation Index Equation and Values Interpretation. Available online: https://eos.com/make-an-analysis/ndmi (accessed on 1 January 2026).
61. Bolton, D.K.; Coops, N.C.; Hermosilla, T.; Wulder, M.A.; White, J.C. Assessing the accuracy of postfire vegetation recovery trajectories derived from Landsat time series. *Remote Sens. Environ.* **2020**, *238*, 111233.
62. Nguyen, T.H.; Jones, S.; Soto-Berelov, M.; Haywood, A.; Hislop, S. Landsat Time-Series for Estimating Forest Aboveground Biomass and Its Dynamics across Space and Time: A Review. *Remote Sens.* **2020**, *12*, 98. [CrossRef]
63. Johnstone, J.F.; Chapin, F.S.; Hollingsworth, T.N.; Mack, M.C.; Romanovsky, V.; Turetsky, M. Fire, climate change, and forest resilience in interior Alaska. *Can. J. For. Res.* **2010**, *40*, 1302–1312. [CrossRef]
64. Meng, R.; Dennison, P.E.; D'Antonio, C.M.; Moritz, M.A. Remote sensing analysis of vegetation recovery following wildfire in southern California. *Remote Sens. Environ.* **2018**, *204*, 250–261.
65. Giglio, L.; Boschetti, L.; Roy, D.P.; Humber, M.L.; Justice, C.O. The Collection 6 MODIS burned area mapping algorithm and product. *Remote Sens. Environ.* **2018**, *217*, 72–85. [CrossRef]
66. Shapiro, S.S.; Wilk, M.B. An analysis of variance test for normality (complete samples). *Biometrika* **1965**, *52*, 591–611. [CrossRef]
67. Levene, H. Robust tests for equality of variances. In *Contributions to Probability and Statistics: Essays in Honor of Harold Hotelling*; Olkin, I., Ed.; Stanford University Press: Stanford, CA, USA, 1960; pp. 278–292.

68. Kruskal, W.H.; Wallis, W.A. Use of ranks in one-criterion variance analysis. *J. Am. Stat. Assoc.* **1952**, *47*, 583–621. [CrossRef]
69. Tukey, J.W. Comparing individual means in the analysis of variance. *Biometrics* **1949**, *5*, 99–114. [CrossRef] [PubMed]
70. Spearman, C. The proof and measurement of association between two things. *Am. J. Psychol.* **1904**, *15*, 72–101. [CrossRef] [PubMed]
71. R Core Team. *R: A Language and Environment for Statistical Computing*; R Foundation for Statistical Computing: Vienna, Austria, 2024; Available online: https://www.R-project.org/ (accessed on 1 January 2026).
72. Neary, D.G.; Klopatek, C.C.; DeBano, L.F.; Ffolliott, P.F. Fire effects on belowground sustainability: A review and synthesis. *For. Ecol. Manag.* **1999**, *122*, 51–71. [CrossRef]
73. DeBano, L.F.; Neary, D.G.; Ffolliott, P.F. *Fire's Effects on Ecosystems*; John Wiley & Sons: New York, NY, USA, 1998.
74. Mataix-Solera, J.; Cerdà, A.; Arcenegui, V.; Jordán, A.; Zavala, L.M. Fire effects on soil aggregation: A review. *Earth-Sci. Rev.* **2011**, *109*, 44–60. [CrossRef]
75. Zar, J.H. *Biostatistical Analysis*, 5th ed.; Pearson Prentice Hall: Upper Saddle River, NJ, USA, 2010.
76. Quinn, G.P.; Keough, M.J. *Experimental Design and Data Analysis for Biologists*; Cambridge University Press: Cambridge, UK, 2002.
77. Wang, S.; Zheng, X.; Du, Y.; Zhang, G.; Wang, Q.; Han, D.; Zhang, J. Estimation of Short-Term Vegetation Recovery in Post-Fire Siberian Dwarf Pine (*Pinus pumila*) Shrublands Based on Sentinel-2 Data. *Fire* **2025**, *8*, 47. [CrossRef]
78. Han, Y.; Wang, X.; Zhou, Y.; Jin, H. Impacts of high-severity fires on soil organic layers and forest regeneration in boreal ecosystems. *For. Ecol. Manag.* **2021**, *496*, 119428.
79. Zahabnazouri, M.; Smith, J.; Allen, C.D. Fire-driven ecosystem reset and limits to forest recovery under climate extremes. *Glob. Change Biol.* **2025**, *31*, e17123.
80. Andrieux, B.; Drobyshev, I.; Niklasson, M. Effects of fire severity on pine regeneration and soil properties. *Ann. For. Sci.* **2018**, *75*, 102.
81. Pinheiro, J.; Moreira, F.; Catry, F.X. Mixed-severity fires promote regeneration heterogeneity in pine ecosystems. *For. Ecol. Manag.* **2025**, *553*, 121679.
82. Braziunas, K.H.; Hansen, W.D.; Harvey, B.J.; Turner, M.G. Fire severity shapes early successional pathways in boreal forests. *Ecol. Appl.* **2023**, *33*, e2823.
83. van Gerrevink, M.J.; Veraverbeke, S.; Cooperdock, S.; Potter, S.; Zhong, Q.; Moubarak, M.; Virkkala, A.-M.; Goetz, S.J.; Mack, M.C.; Randerson, J.T.; et al. Climate impacts from North American boreal forest fires. *Nat. Geosci.* **2026**, *19*, 455–461. [CrossRef]
84. Whitman, E.; Parisien, M.-A.; Thompson, D.K.; Flannigan, M.D. Short-interval wildfire and drought overwhelm boreal forest resilience. *Sci. Rep.* **2019**, *9*, 18796. [CrossRef]
85. Kharuk, V.I.; Ranson, K.J.; Im, S.T.; Dvinskaya, M.L. Wildfires in northern Siberian larch dominated communities. *Environ. Res. Lett.* **2016**, *11*, 045017. [CrossRef]
86. Downing, W.M.; Krawchuk, M.A. Fine-scale fire heterogeneity influences forest resilience. *Glob. Ecol. Biogeogr.* **2019**, *28*, 497–509.
87. Parks, S.A.; Holsinger, L.M.; Panunto, M.H.; Jolly, W.M.; Dobrowski, S.Z.; Dillon, G.K. High-severity fire: Evaluating its key drivers and mapping its probability across western US forests. *Environ. Res. Lett.* **2018**, *13*, 044037. [CrossRef]
88. McNamara, N.P.; Black, H.I.J.; Beresford, N.A.; Parekh, N.R. Soil organic matter dynamics following wildfire. *Soil Biol. Biochem.* **2019**, *135*, 72–82.
89. Yıldız, O.; Sarginci, M.; Esen, D. Postfire soil chemistry and seedling establishment. *Eur. J. For. Res.* **2023**, *142*, 125–139.
90. Hu, K.; Zhang, E.; Dai, X.; Xia, M.; Zhou, F.; Weng, L.; Lin, H. MCSGNet: A Encoder–Decoder Architecture Network for Land Cover Classification. *Remote Sens.* **2023**, *15*, 2810. [CrossRef]
91. Kurbanov, E.A.; Vorobyev, O.Y.; Gafarov, A.K. Effects of high-intensity fires on soil properties and forest regeneration in boreal Eurasia. *J. Environ. Manag.* **2022**, *301*, 113877.
92. Parker, T.J.; Clancy, K.M.; Mathiasen, R.L. Interactions among fire, insects and pathogens in coniferous forests of North America. *Agric. For. Entomol.* **2015**, *17*, 167–189.
93. Seidl, R.; Turner, M.G. Post-disturbance reorganization of forest ecosystems in a changing world. *Proc. Natl. Acad. Sci. USA* **2022**, *119*, e2202190119. [CrossRef]

Disclaimer/Publisher's Note: The statements, opinions and data contained in all publications are solely those of the individual author(s) and contributor(s) and not of MDPI and/or the editor(s). MDPI and/or the editor(s) disclaim responsibility for any injury to people or property resulting from any ideas, methods, instructions or products referred to in the content.